

Computational Deep Learning Microscopy

Presented by:





COMPUTATIONAL DEEP LEARNING MICROSCOPY WEBINAR

21 March 2019 • 14:00 EDT

OSA Photonic
Detection
Technical Group



Speaker: Prof. Yair Rivenson
UCLA



Committee 2019



Girija Gaur

Chair

Kramer Levin Naftalis & Frankel



Achyut Dutta

Vice Chair

Founder Banpil Photonics



Shuren Hu

Events Officer US/Asia/EU

GlobalFoundries



Chi Xiong

Events Officer US

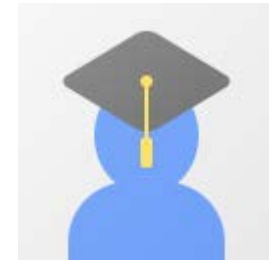
IBM



Gabe Spalding

Member

Illinois Wesleyan University



Rajan Jha

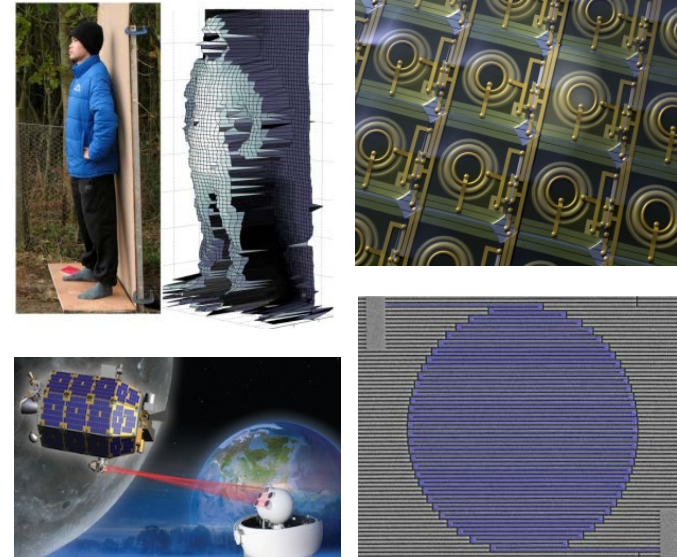
Events Officer India

IIT Bhubaneswar, India

About Us

The Photonic Detection technical group is part of the Photonics and Opto-Electronics Division of the Optical Society. This group focuses on the detection of photons as received from images, data links, and experimental spectroscopic studies to mention a few. Within its scope, the PD technical group is involved in the design, fabrication, and testing of single and arrayed detectors.

This group focuses on materials, architectures, and readout circuitry needed to transduce photons into electrical signals and further processing. This group's interests include: (1) the integration of lens, cold shields, and readout electronics into cameras, (2) research into higher efficiency, lower noise, and/or wavelength tunability, (3) techniques to mitigate noise and clutter sources that degrade detector performance, and (4) camera design, components, and circuitry.



Find us online

OSA Homepage

www.osa.org/PD

LinkedIn Group

www.linkedin.com/groups/8297763



[About OSA](#) [Awards](#) [Career](#) [Video](#)

Journals & Proceedings

Meetings & Exhibits

Celebrating 100 Years

Explore Membership

Industry Programs

Get Involved

Home / Get Involved / Technical Divisions / Photonics and Opto-Electronics

Photonic Detection (PD)

Get Involved

Technical Divisions +

Bio-Medical Optics

Fabrication, Design & Instrumentation

Information Acquisition, Processing & Display

Optical Interaction Science

Photonics and Opto-Electronics +

Fiber Optics Technology (PF)

Integrated Optics (PI)

Laser Systems (PL)

Optical Communications (PC)

Photonic Detection (PD)



This group involves the detection of photons as received from images, data links, and experimental spectroscopic studies to mention a few. Within its scope, it is involved in the design, fabrication, testing of single and arrayed detectors. Detector materials, structures, and readout circuitry needed to translate photons into electrical signals are considered by this group. Also included in this group is the integration of components such as lens, cold shields, and readout electronics into cameras. Research into higher efficiency, lower noise, and/or wavelength tunability is included here. Additionally, techniques to mitigate noise and clutter sources that degrade detector performance are within the purview of this group. In the imaging area, camera design, componentry, and circuitry are considered.

Announcer

Join the Photonic D Group for their ina Wednesday, 27 Apr

In this webinar, Dr. describe his recent speed quantum ke photonic integrate scalable quantum i processors based c networks.

[Register for the W](#)

Technical Group Activities

- **Special Sessions** at OSA conferences such as CLEO and OFC.
- **~4 Webinars** for this year!
- Interactions with local sections and student chapters.
- Interactive community for bringing together researchers across interdisciplinary fields for tackling advances in photonic detection technologies.
- Example: Panel discussion on ***Silicon Photonics for LiDAR and Other Applications*** at OFC 2019 which had great turn-out and a lot of interest!



Computational Deep Learning Microscopy

Yair Rivenson

Electrical and Computer Engineering Department

UCLA

OSA Webinar

March 21st, 2019

Optica 4, 1437-1443 (2017)

Light Sci. Appl. 7, e17141 (2018)

ACS Photonics (2018), DOI: 10.1021/acsp Photonics.8b00146

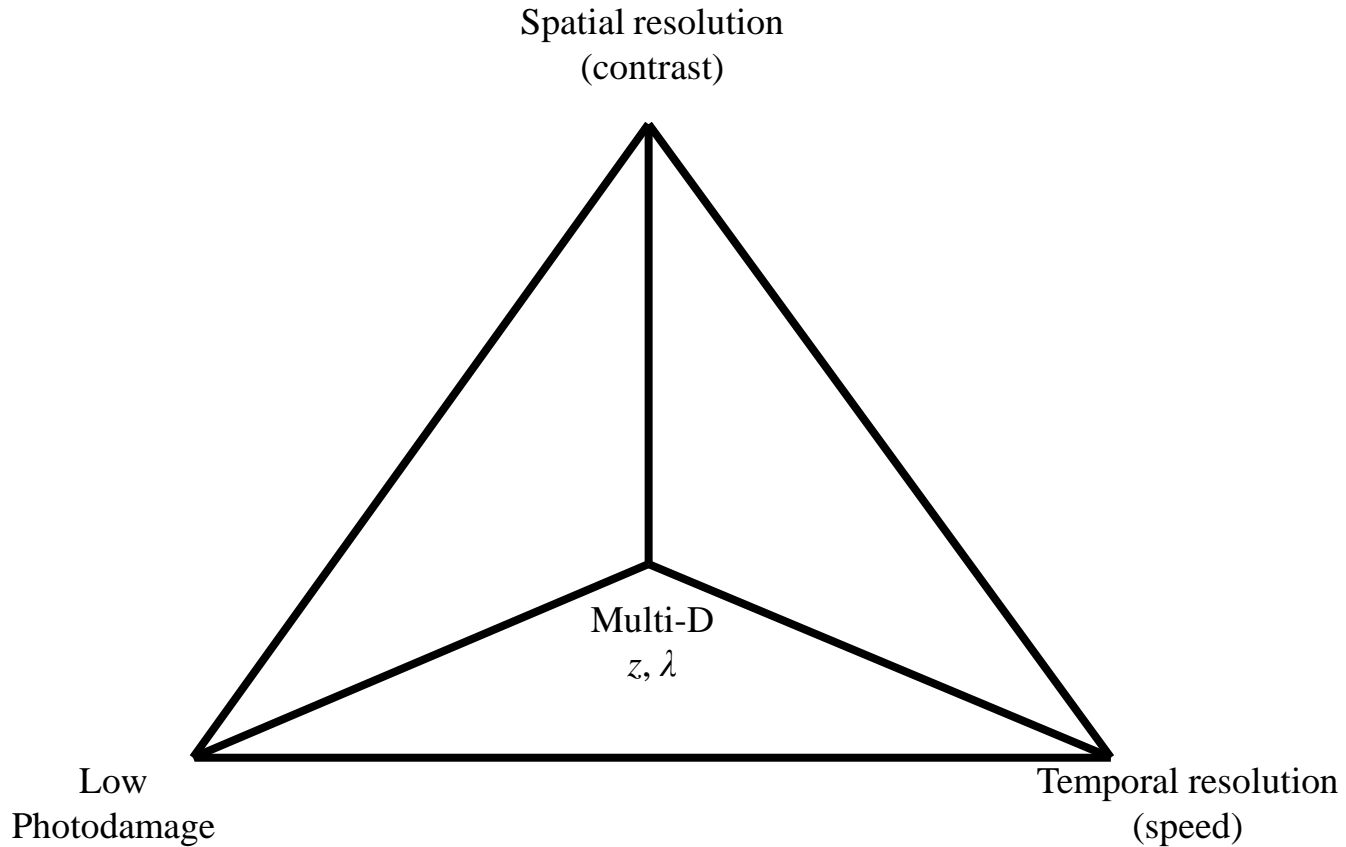
Nat. Methods 16, 103 (2019)

Nat. Biomed. Eng. 1 (2019). doi:10.1038/s41551-019-0362-y

Light Sci. Appl. 8, 23 (2019)

Light Sci. Appl. 8, 25 (2019)

Tradeoffs in microscopy



Computational microscopy



- Using a numerical model of the imaging system to computationally estimate the underlying object model.

Computational microscopy - inverse problems

- Reconstruction (dense prediction): $p(\mathbf{x}|\mathbf{y})$

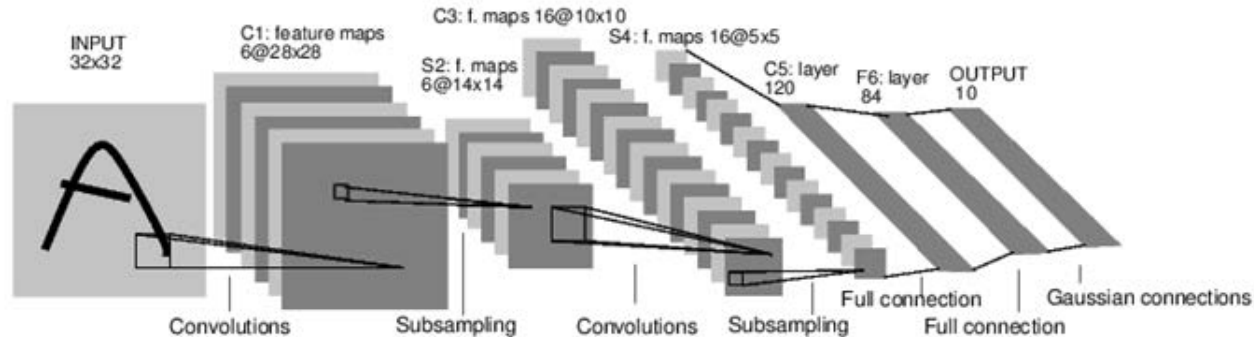
$$p(\mathbf{x}|\mathbf{y}) = \frac{p(\mathbf{y}|\mathbf{x})p(\mathbf{y})}{p(\mathbf{x})}$$

- Leads to linear / non-linear estimators:

$$\mathbf{x}_e = \arg \min_{\mathbf{x}_e} \|\mathbf{y} - H\mathbf{x}_e\|_2^2 + \lambda\phi(\mathbf{x}_e)$$

- H – forward operator, measurement model.
- $\phi(\cdot)$ – Prior information on the object (sparsity, non-negativity, support, ...).
- λ – Regularization parameter.

Deep convolutional neural network



A Full Convolutional Neural Network (LeNet)

- Deep convolutional neural network implement functions by solving an optimization problem.

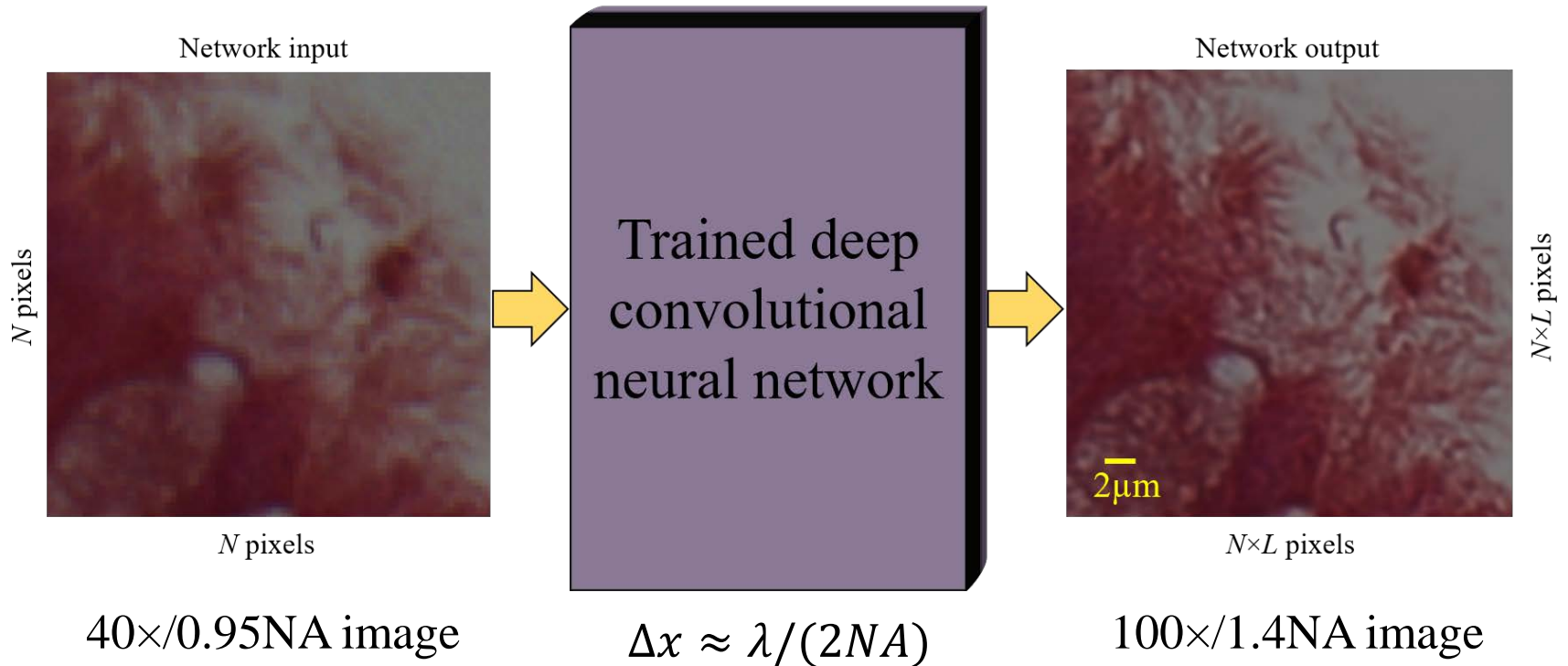
$$f(y) = O_n A_n \cdots O_2 A_2 \cdot O_1 A_1 y$$
- Optimized only once and remains fixed.
- Reconstruction performed in a single feed-forward step.

LeCun, Y., et al., "Gradient-based learning applied to document recognition," Proceedings of the IEEE, Nov. 1998.

LeCun, Y., Bengio, Y. & Hinton, G., "Deep learning," Nature 521, 436–444 (2015).

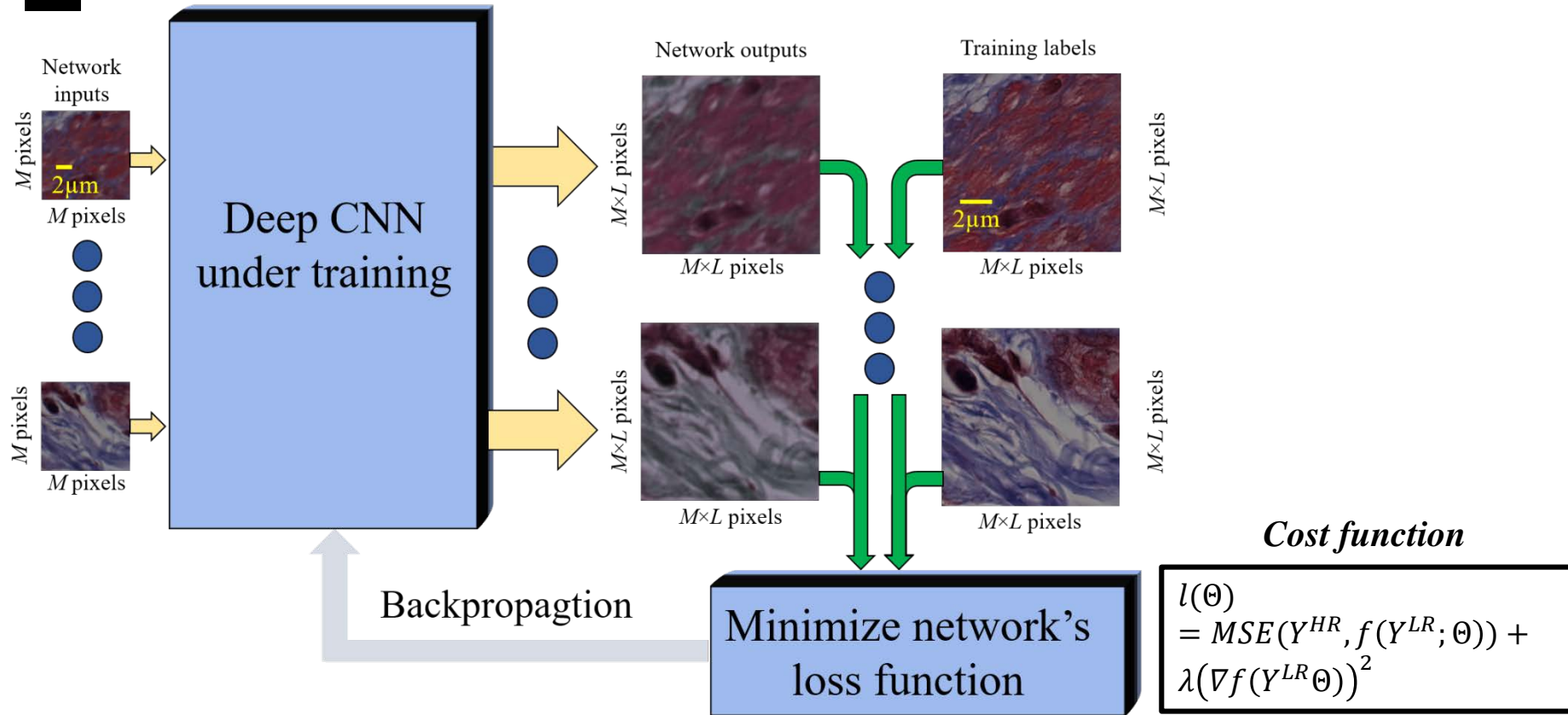
Schmidhuber, J., "Deep learning in neural networks: An overview. Neural Netw.," 61, 85–117 (2015).

Deep learning microscopy



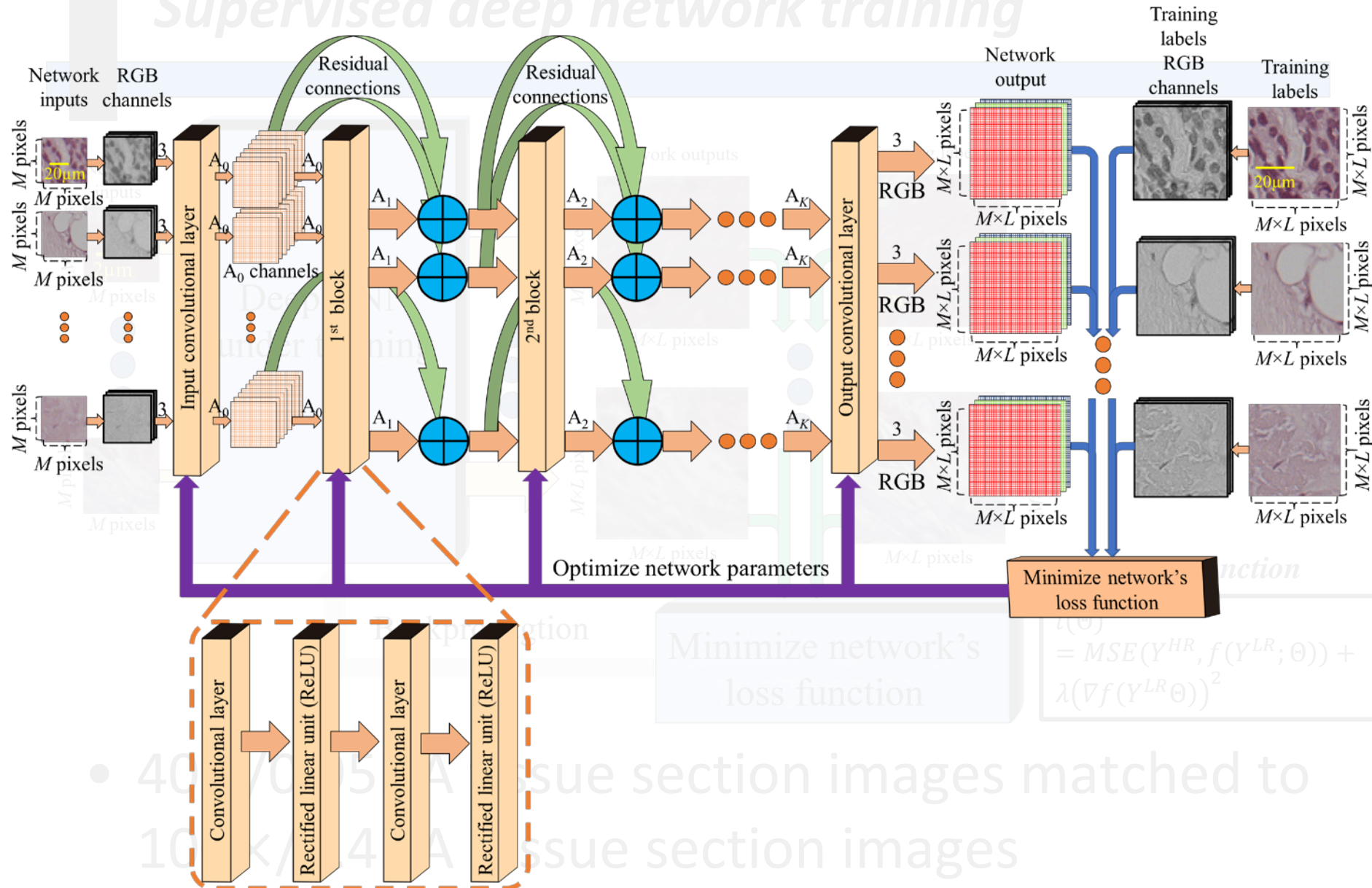
- Works with standard microscope hardware.
- Towards real time performance,
- Do not use forward models.

Supervised deep network training

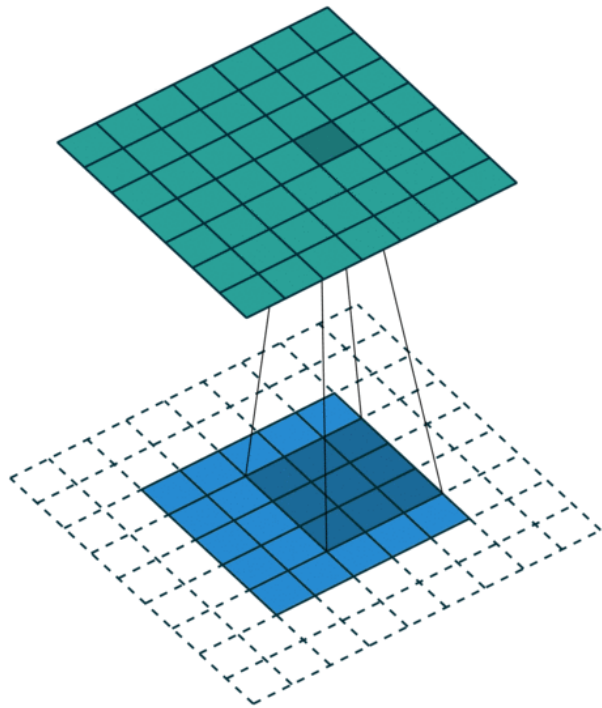


- 40×/0.95NA tissue section images matched to 100×/1.4NA tissue section images (brightfield microscopy).

Supervised deep network training



- 40x/70x/15x A tissue section images matched to 10x/4x A tissue section images (brightfield microscopy).



Convolutional filtering

- *Filter size (throughout the network) – 3×3*

$$v_{i,j}^{k,l} = \sum_r \sum_p \sum_q w_{i,j,r}^{p,q} v_{i-q,j}^{k+p,l+q} + b_{i,j}$$

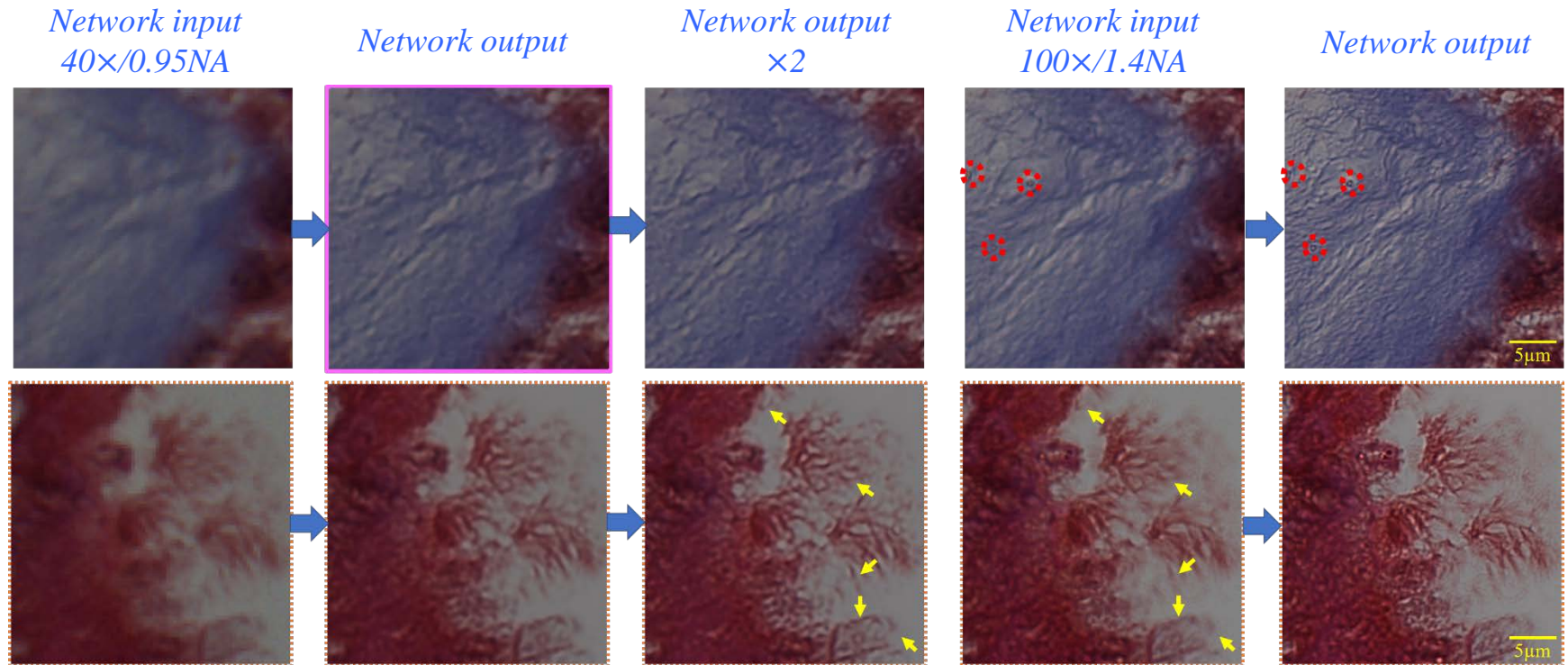
- *Activation function – Rectified Linear Unit - $ReLU(x) = \max(0,x)$*
- *Number of learnable parameters $\sim 230K$*
- *Number of layers = 13*

Implementation details

- Preprocessing – before training, the low resolution and high resolution images were accurately registered.
- Training time \sim 4.5 hours (630 epochs)–
 - 9,536 patches (60 \times 60 pixels) \rightarrow (150 \times 150 pixels).
- Inference time $<$ 1 sec on a dual GPU laptop for a 40 \times objective field-of-view.



Resolution enhancement

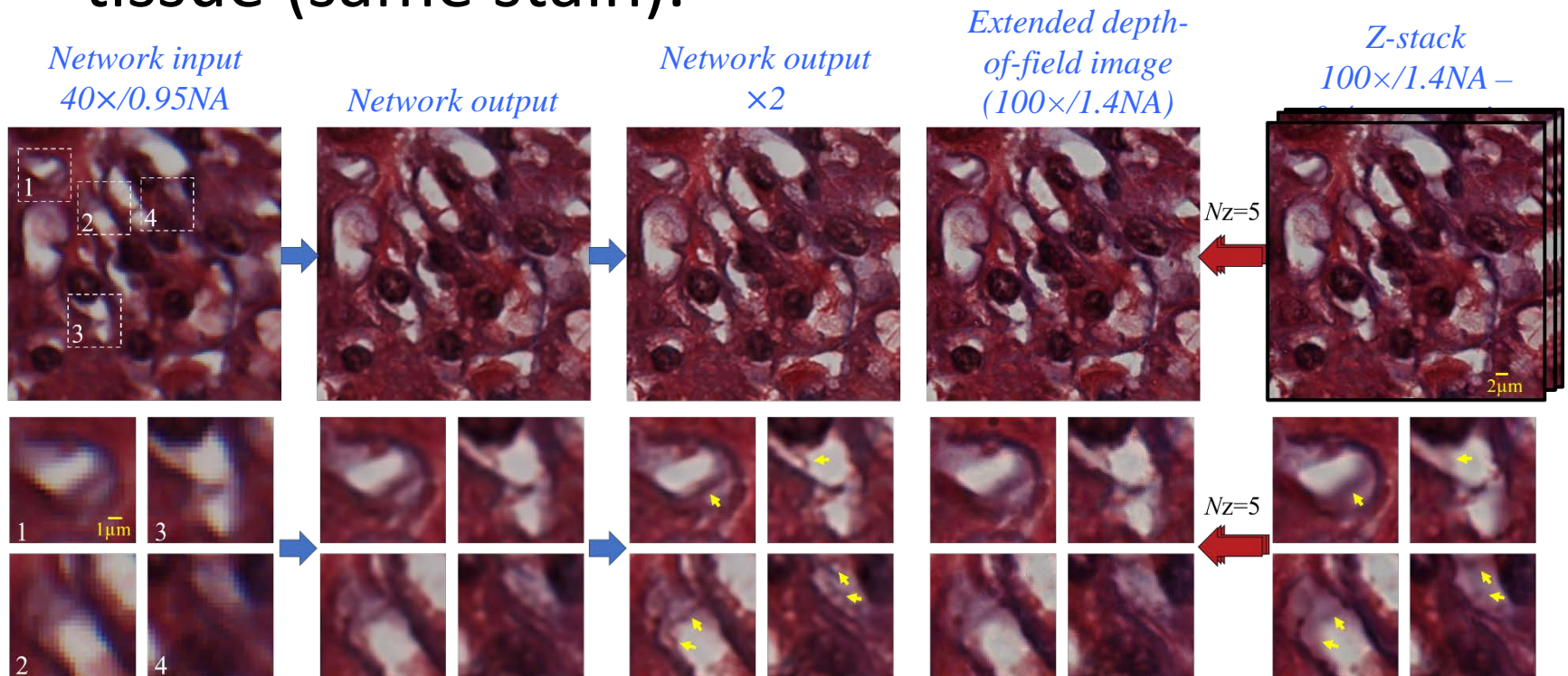


- The image is enhanced while keeping the original field-of-view (>6-fold the field-of-view of the 100x objective).

Extended depth-of-field and cross-tissue

$$\text{depth of field} \approx \lambda/NA^2$$

- Trained on lung tissue, inferred on kidney tissue (same stain).

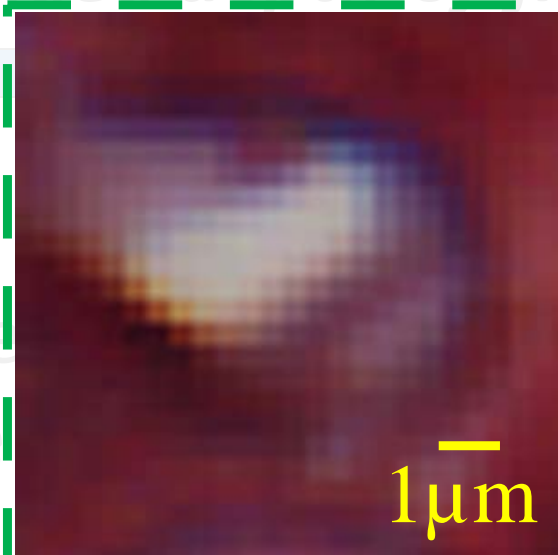


Network input - 40×/0.95NA

Extended depth-of-field and cross-tissue

- Trained
tissue

Network input
40×/0.95NA



Z-stack
100×/1.4NA

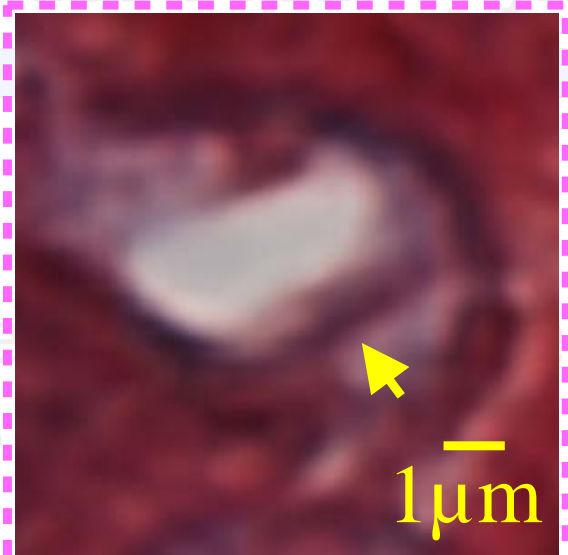


Network output $\times 2$

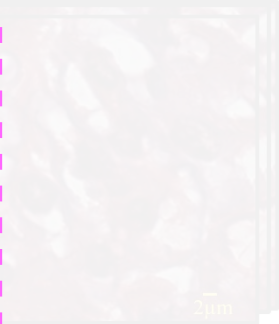
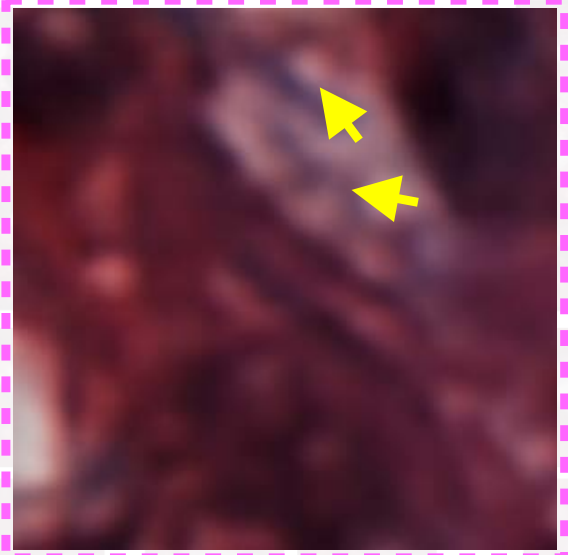
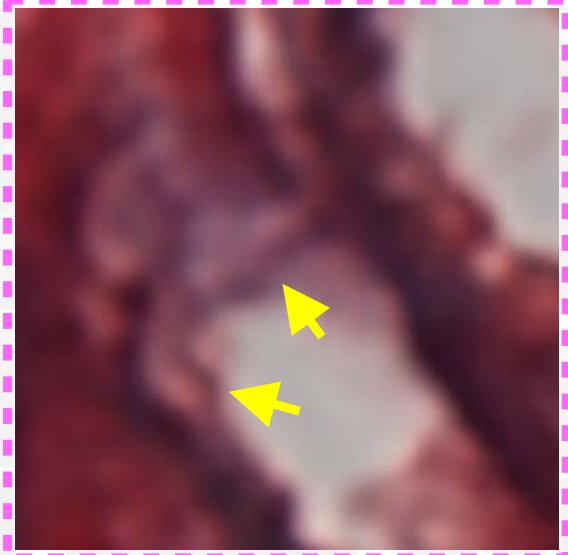
Extended depth-of-field and cross-tissue

- Trained on tissue

Network input
40 \times /0.95NA



Z-stack
100 \times /1.4NA

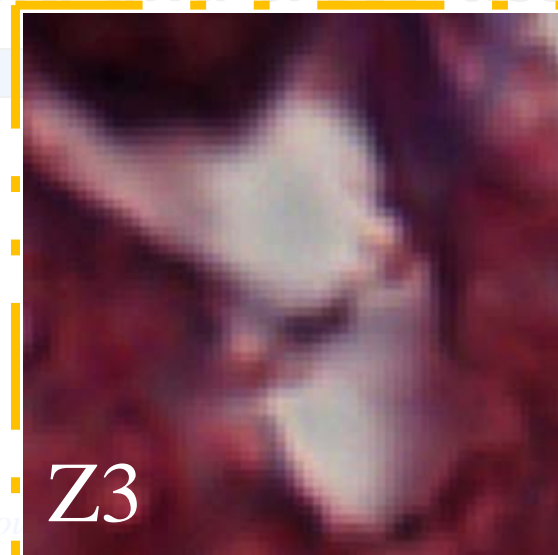
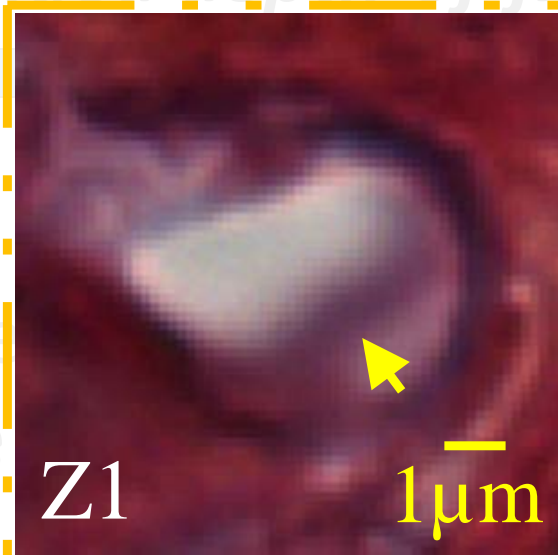


Z-stack (100×/1.4NA): $\Delta z = 0.4\mu\text{m}$

Extended depth-of-field and cross-tissue

- Trained
tissue

Network input
40×/0.95NA



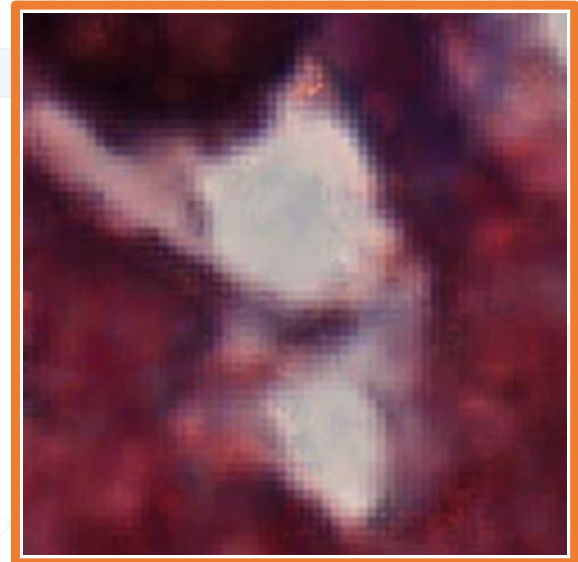
Z-stack
100×/1.4NA

Extended depth-of-field image (100×/1.4NA)

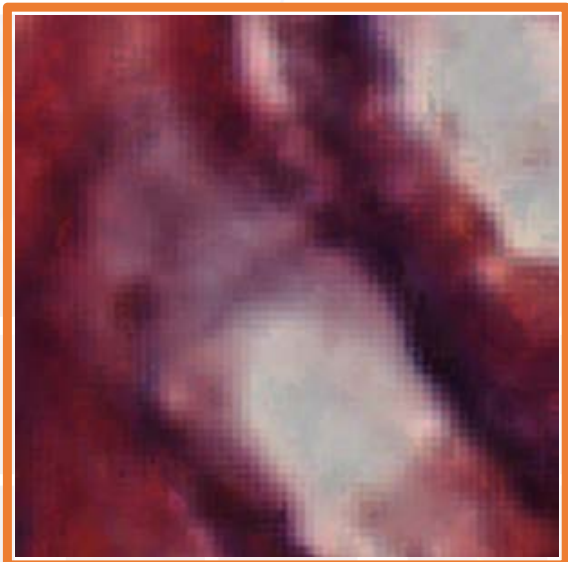
Extended depth-of-field and cross-tissue

- Trained
tissue

Network input
40×/0.95NA

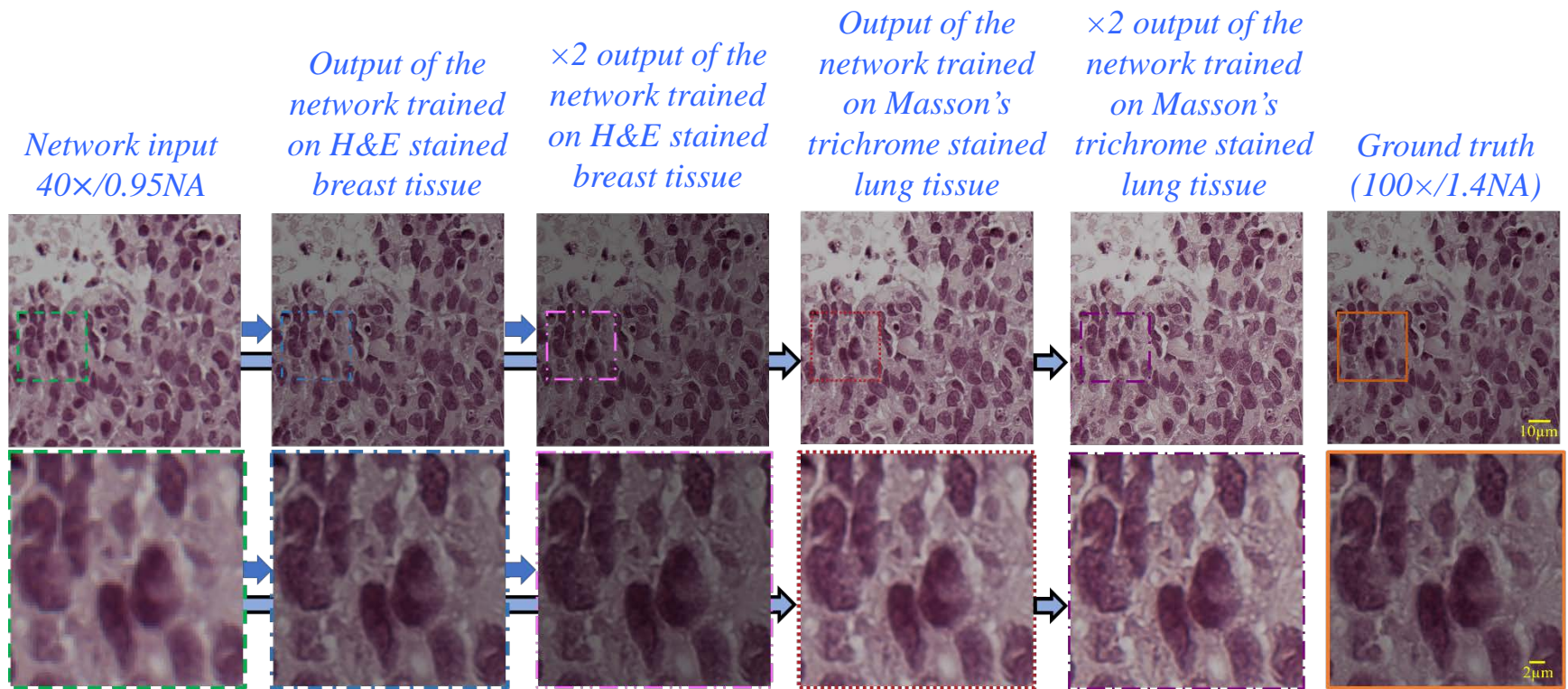


Z-stack
100×/1.4NA



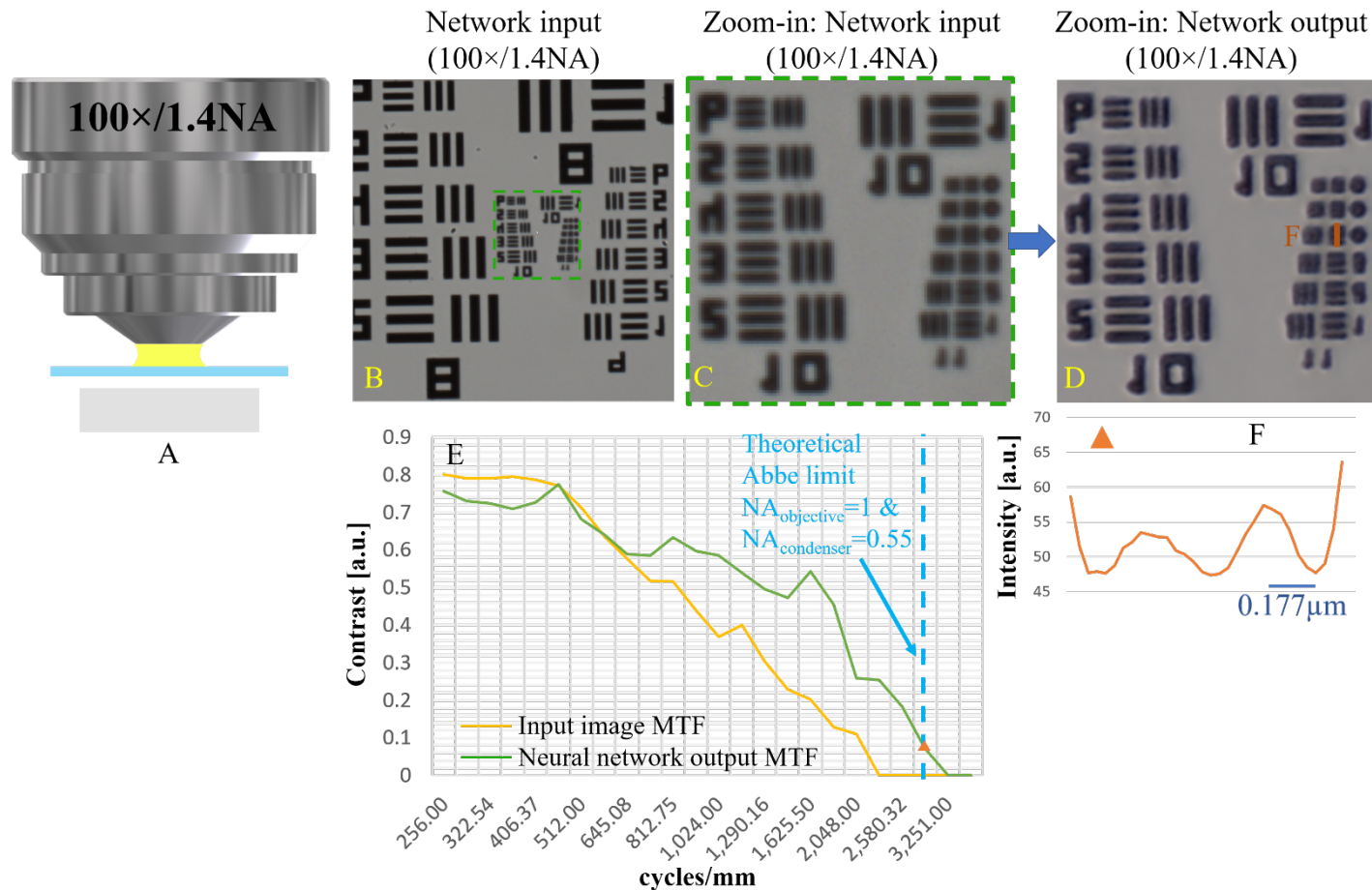
Cross tissue and cross staining

- Trained on lung tissue, inferred on breast tissue, with different stain.



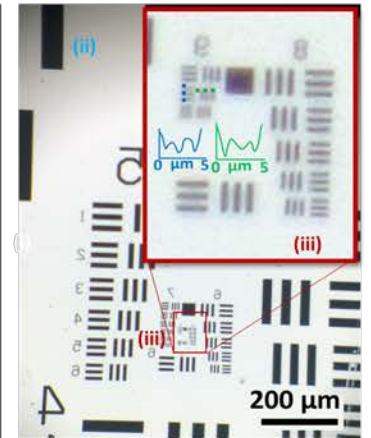
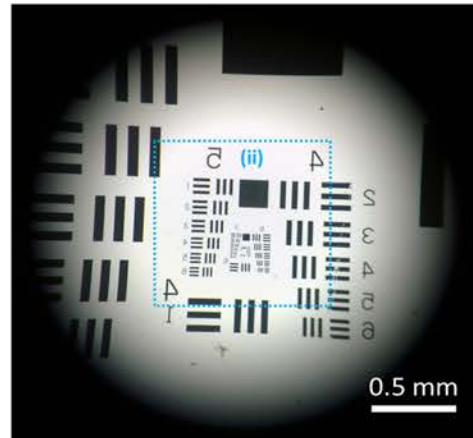
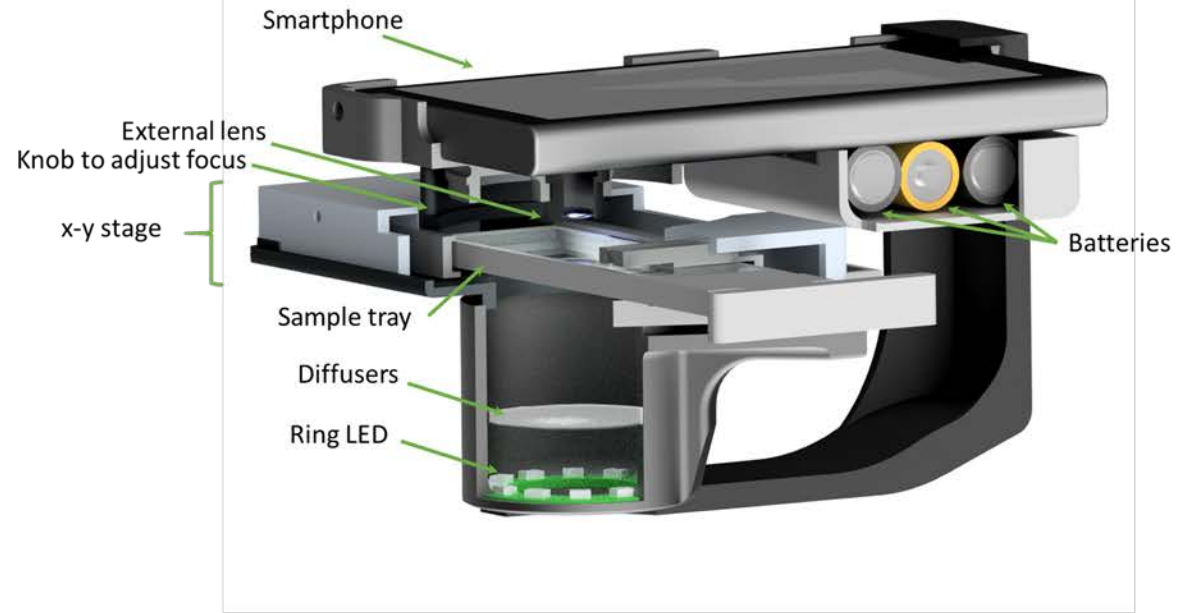
Modulation transfer function estimation

- Network trained with lung tissue.





DEEP LEARNING ENHANCED MOBILE-PHONE MICROSCOPY

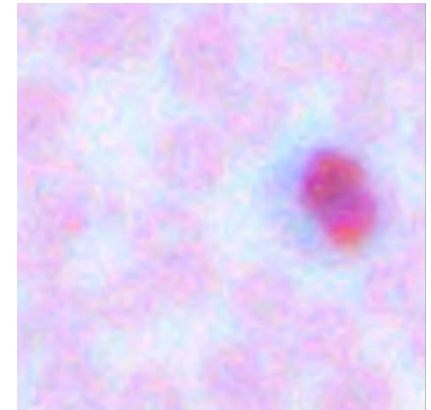


Resolution ~ 0.87μm (half pitch)
FOV ~ 1mm²

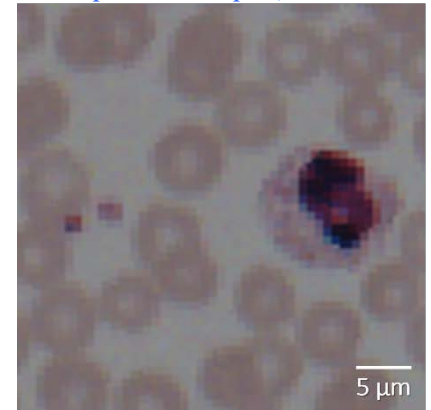
Challenges in mobile microscopy

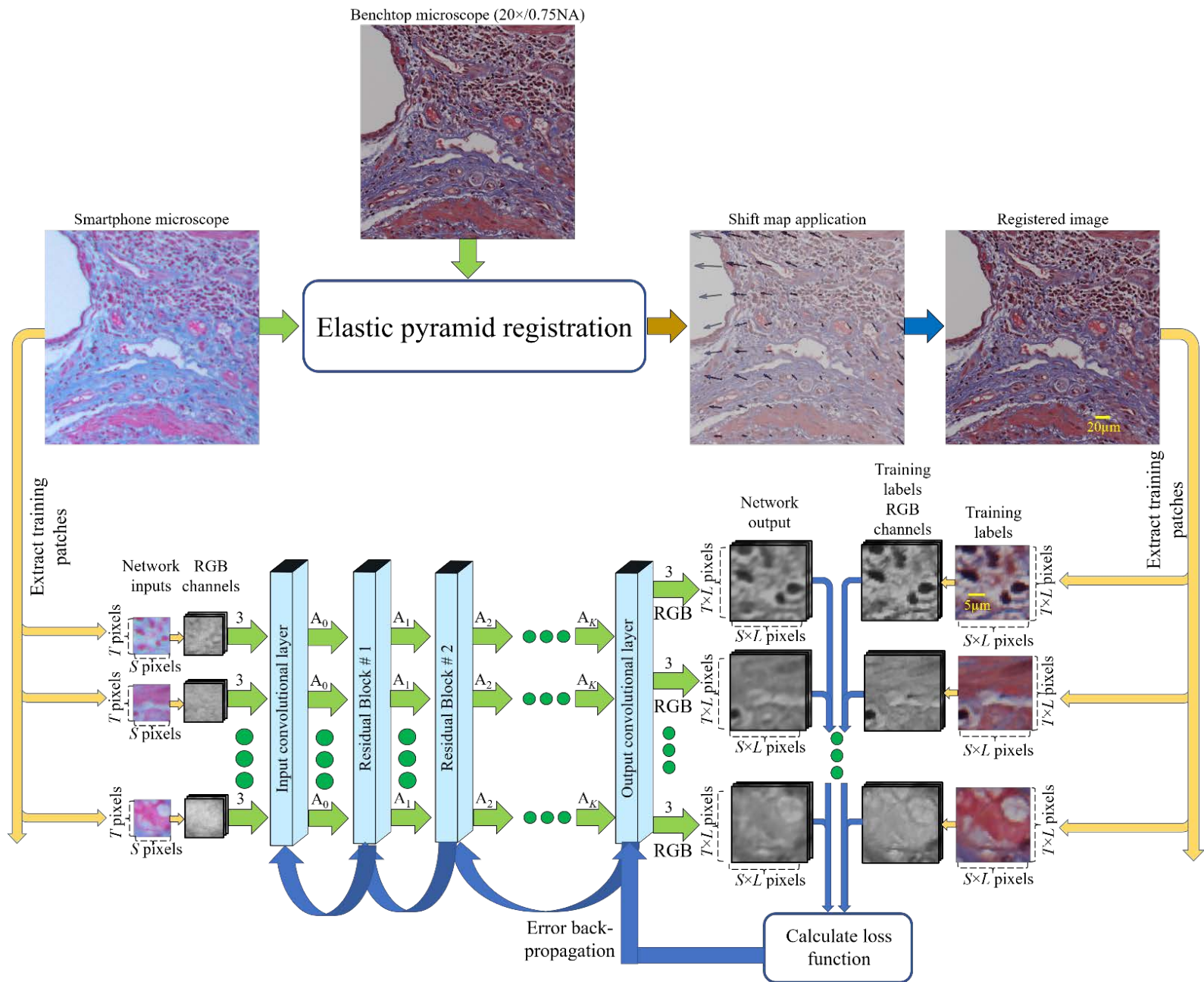
- Main challenge: keep the design cost-effective and portable.
 - Non-optimized, often battery powered illumination.
 - Spectral distortions.
 - SNR due to the pixel size.
 - Spatial aberrations.
 - Lack of mechanical stability.

Smartphone microscope



Benchmark microscope (20×/0.75NA)

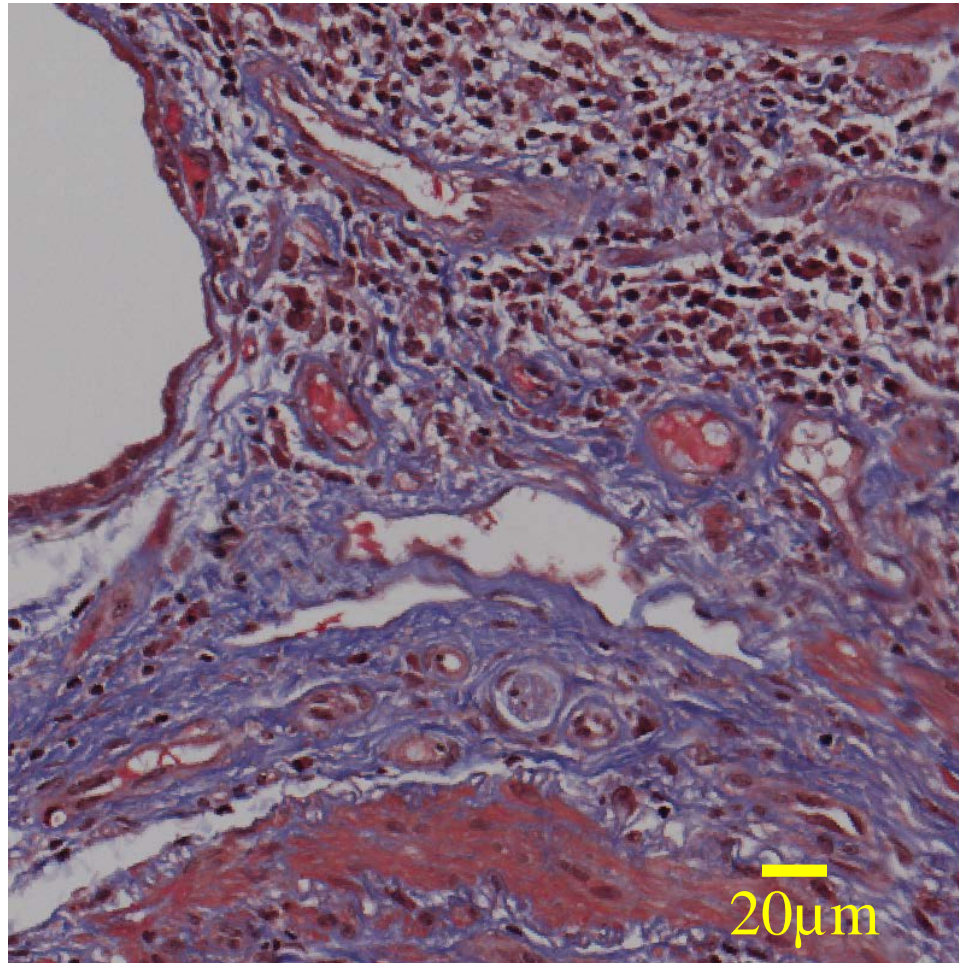




Loss function:
$$l(\Theta) = \text{MSE}(Y^{HR}, f(Y^{LR}; \Theta)) + \lambda(\nabla f(Y^{LR}; \Theta))^2$$

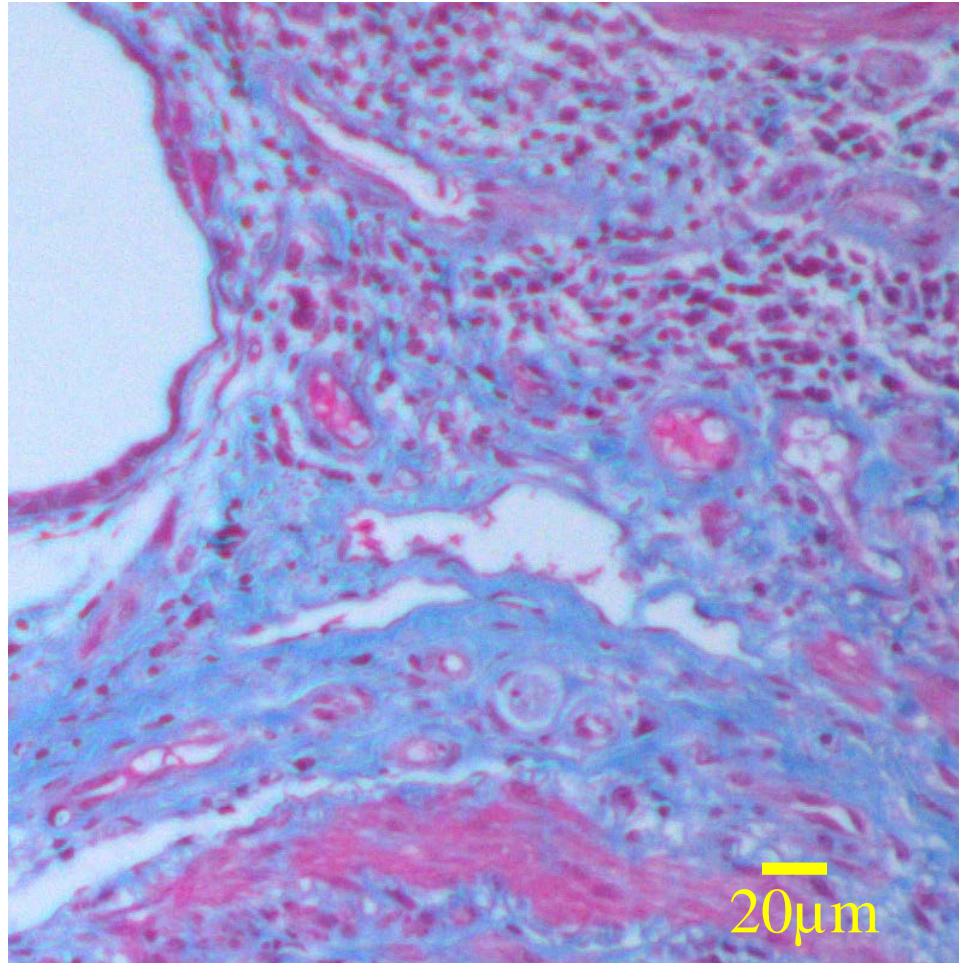
Elastic pyramid registration

Benchtop microscope (20×/0.75NA)



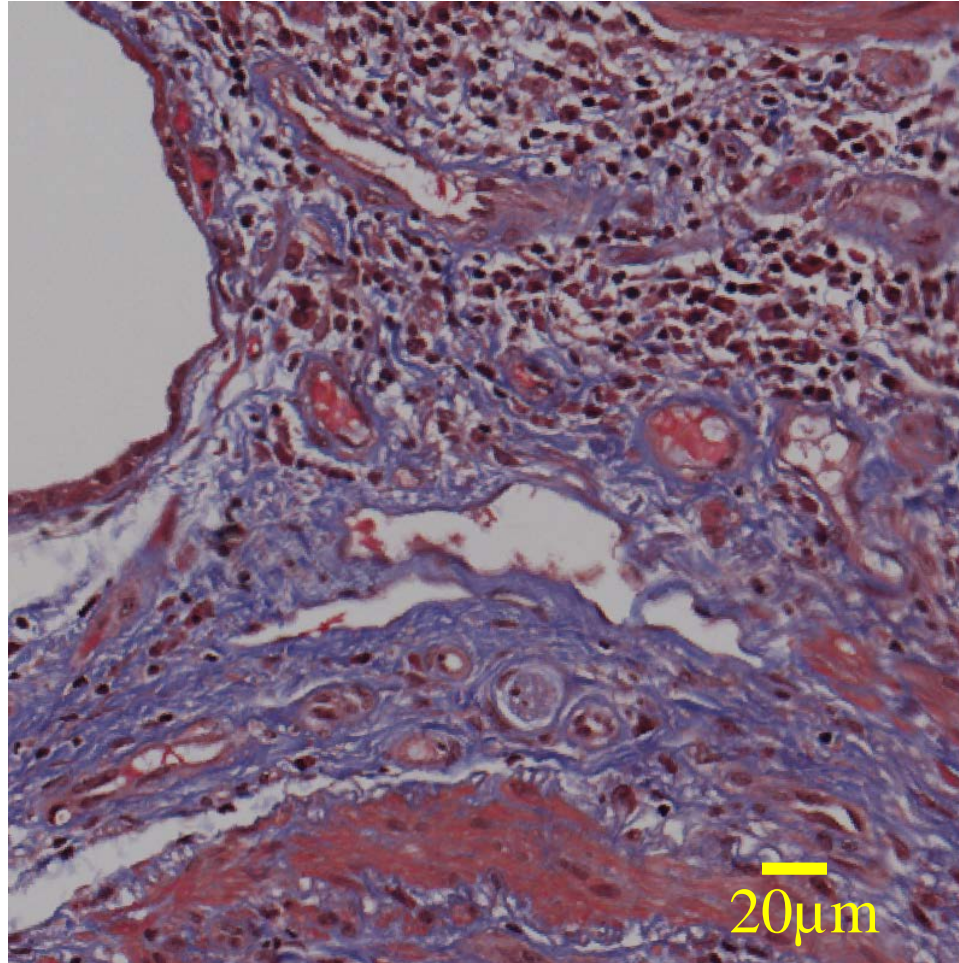
Elastic pyramid registration

Smartphone microscope

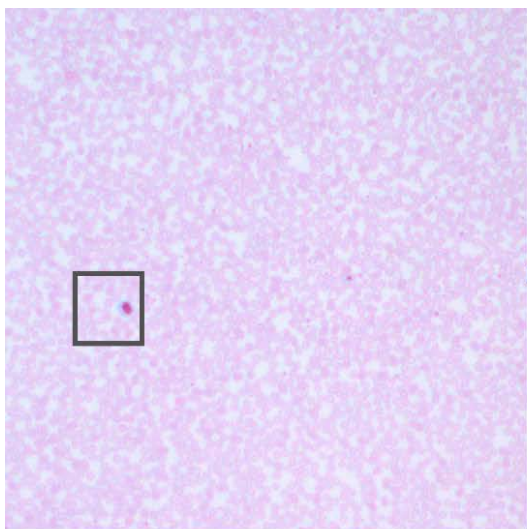


Elastic pyramid registration

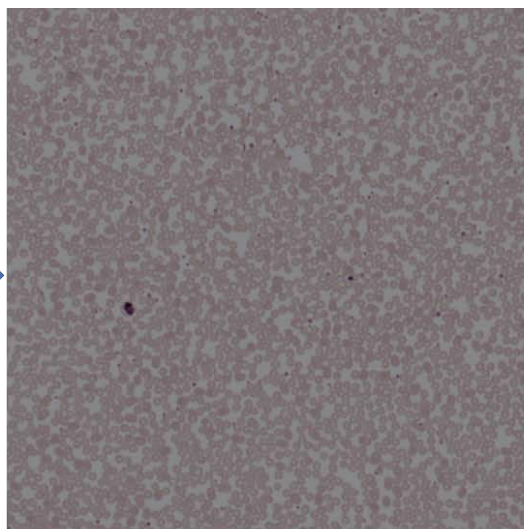
Distortion aligned benchtop microscope image



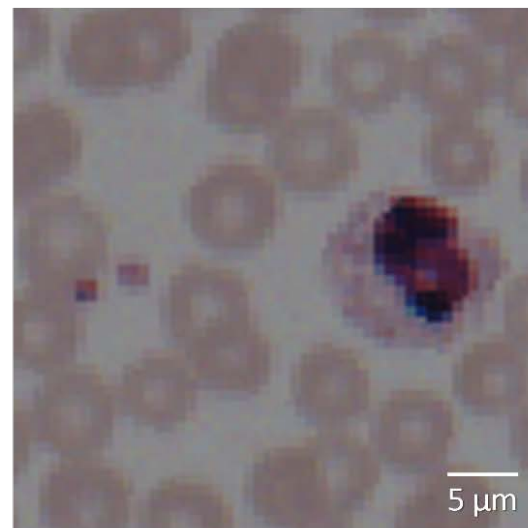
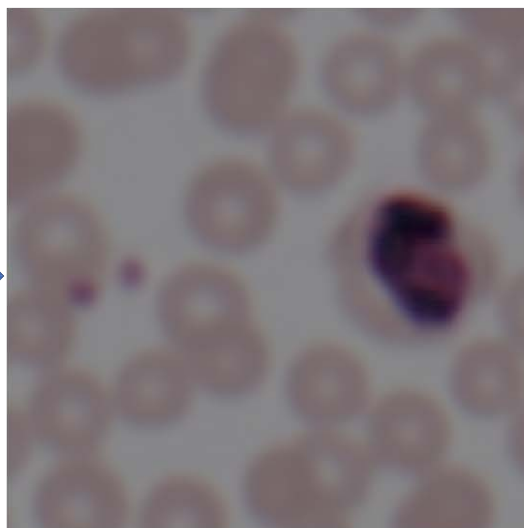
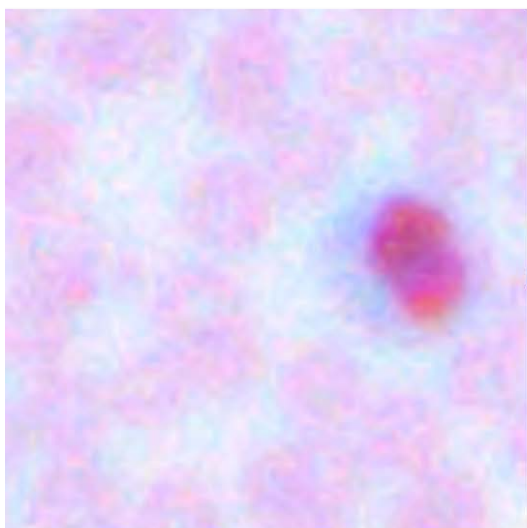
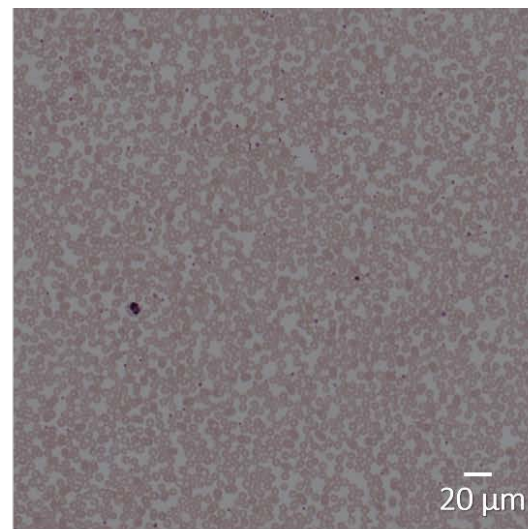
Smartphone microscope



Network output



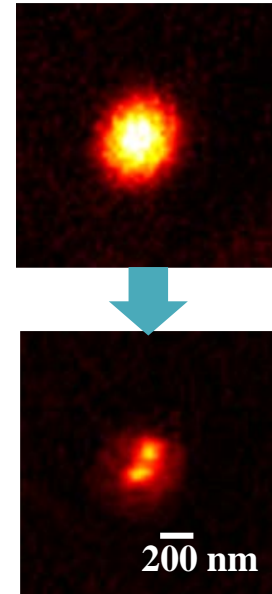
Benchtop microscope (20×/0.75NA)



Structural similarity ~ 0.9

$$SSIM(U_1, U_2) = \frac{(2\mu_1\mu_2+c_1)(2\sigma_{1,2}+c_2)}{(\mu_1^2+\mu_2^2+c_1)(\sigma_1^2+\sigma_2^2+c_2)}; \mu_{1;2} = E[U_{1;2}]; \sigma_{1;2}^2 = E[(U_{1;2} - \mu_{1;2})^2]; \sigma_{1,2} = E[(U_1 - \mu_1)(U_2 - \mu_2)]$$

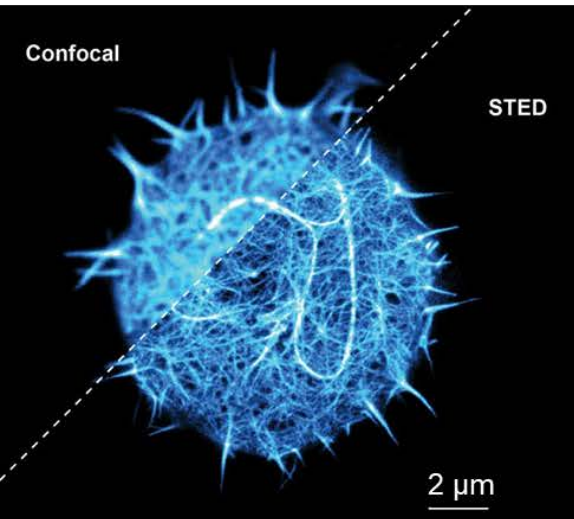
c_1, c_2 : stabilization parameters



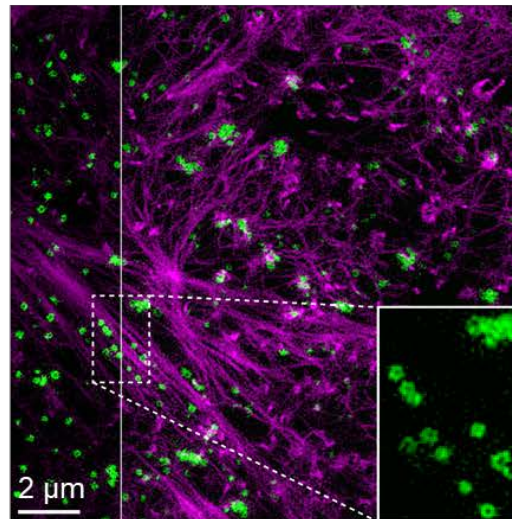
DEEP LEARNING ACHIEVES SUPER-RESOLUTION IN FLUORESCENCE MICROSCOPY

Super-resolution fluorescence microscopy

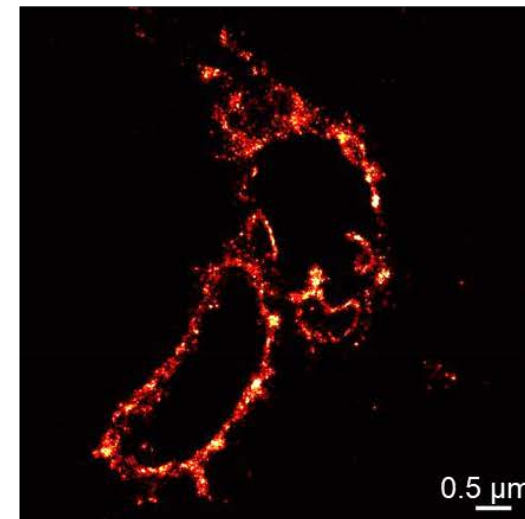
STED¹



SIM²

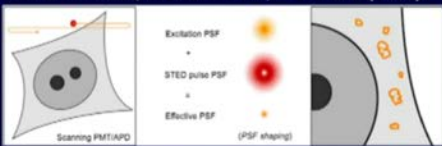
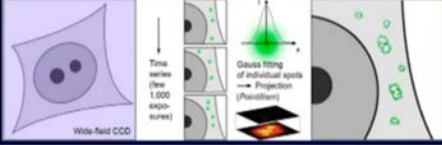
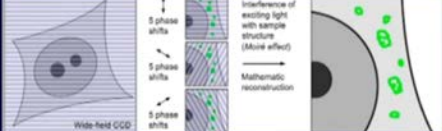


PALM/STORM²



- Provide unprecedented access to the inner working of cells and various biological processes
- Often rely on relatively sophisticated optical setups and extensive computational processing of the image data.

Deep learning enables super-resolution

	reported resolution (nm)	photon increase req'd	intensity (W/cm ²)	acquisition time (sec)
STED / RESOLFT L. Schermelleh, R. Heintzmann, <i>J. Cell Biol.</i> (2010) 	xy: 20 nm xyz: 30 nm	100 1,070	$10^4 - 10^3$	> 60 ~1,000
Localization 	xy: 20 nm xy: 10 nm, z: 20 nm	100 14,400	$10^3 - 10^4$	>20 1,500
SIM 	xy: 100 nm xy: 100 nm, z: 370 nm	4 8	$10 - 10^2$	0.1 - 1 ~10

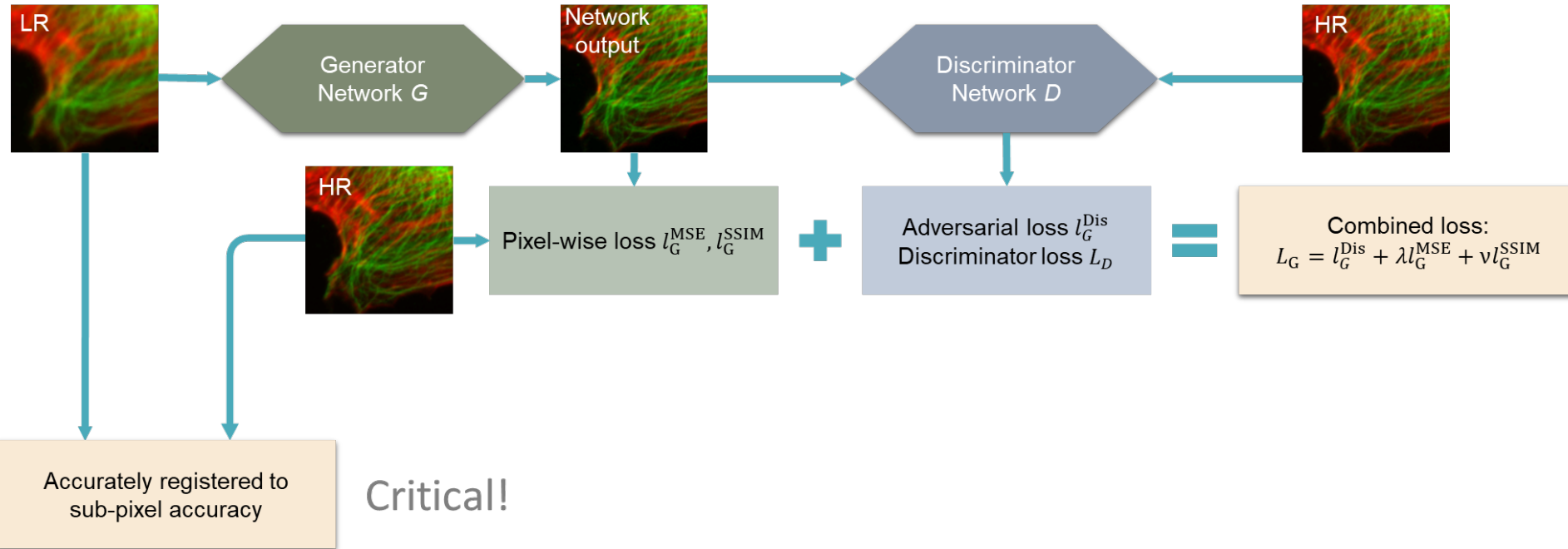
Purposed deep-learning-based approach:

- Network input:
 - Low-resolution image (i.e., captured with low-NA objective)
- Network output:
 - High-resolution image (i.e., captured with high-NA objective)
- Data-driven approach: does not rely on image formation models
- Extended depth-of-field & improved SNR

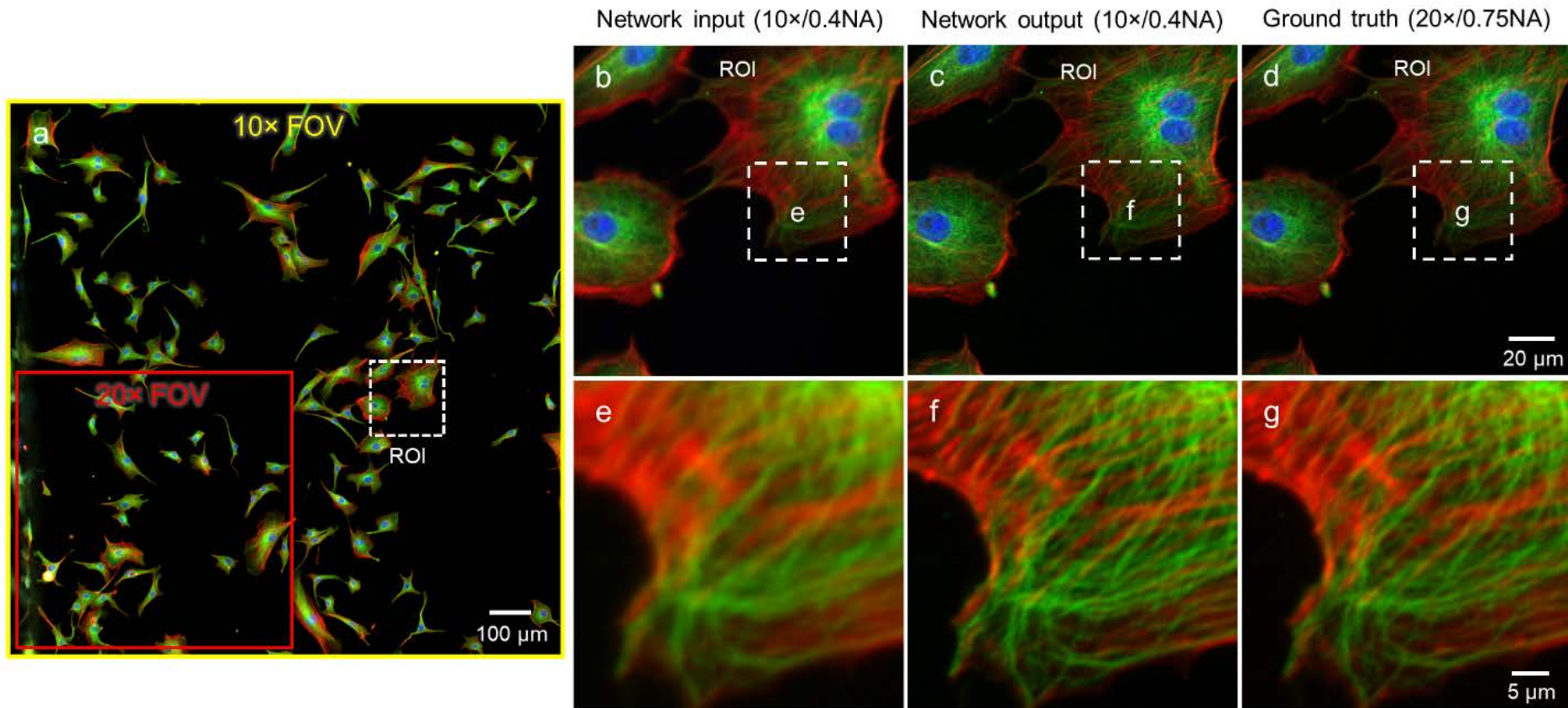
- Major super-resolution techniques introduce extensive photo-toxicity/damage to living samples.¹

¹Eric Betzig: Imaging Life at High Spatiotemporal Resolution

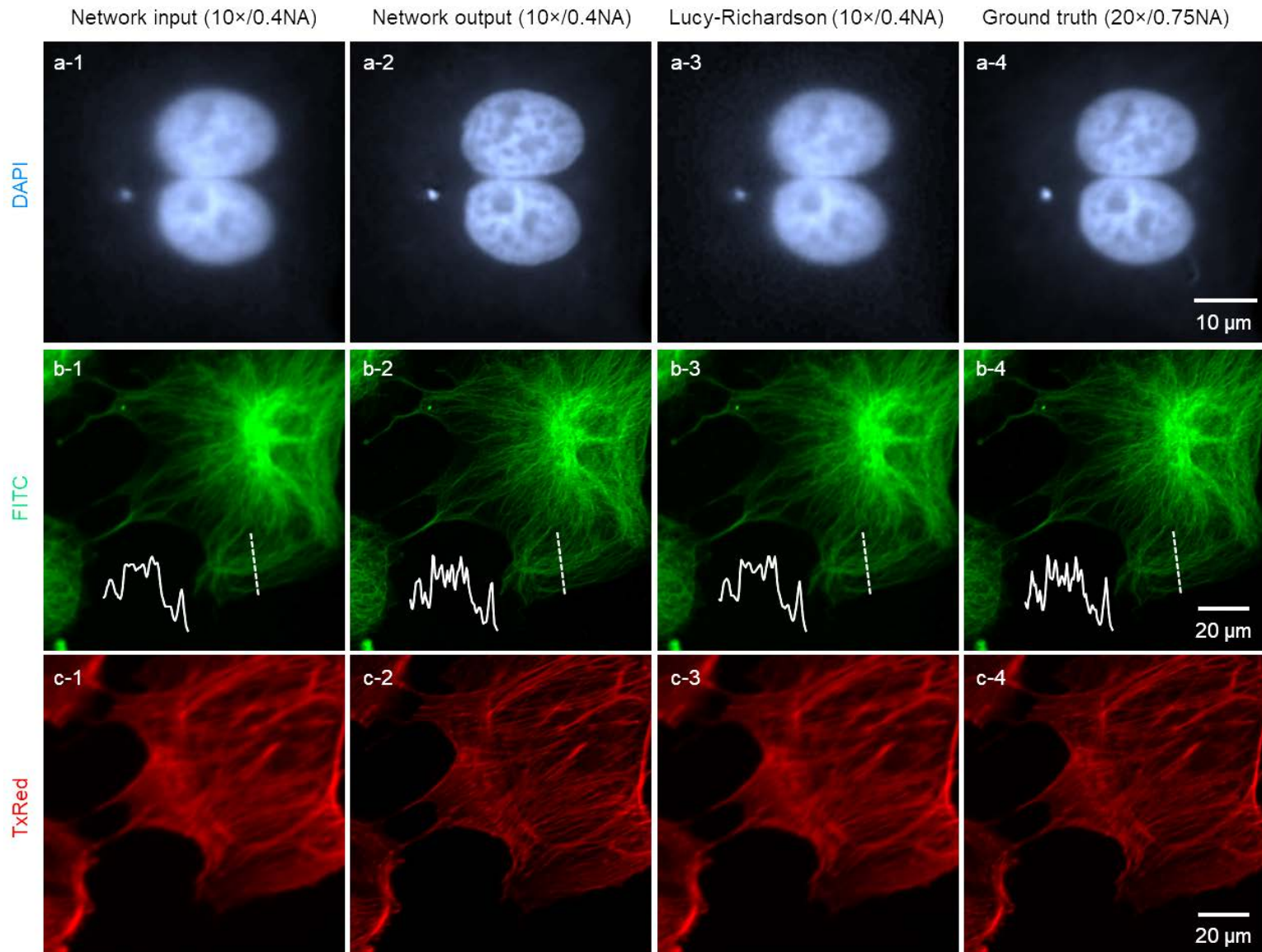
Training workflow of the neural network model



Fluorescence microscopy super-resolution



Fluorescence microscopy super-resolution

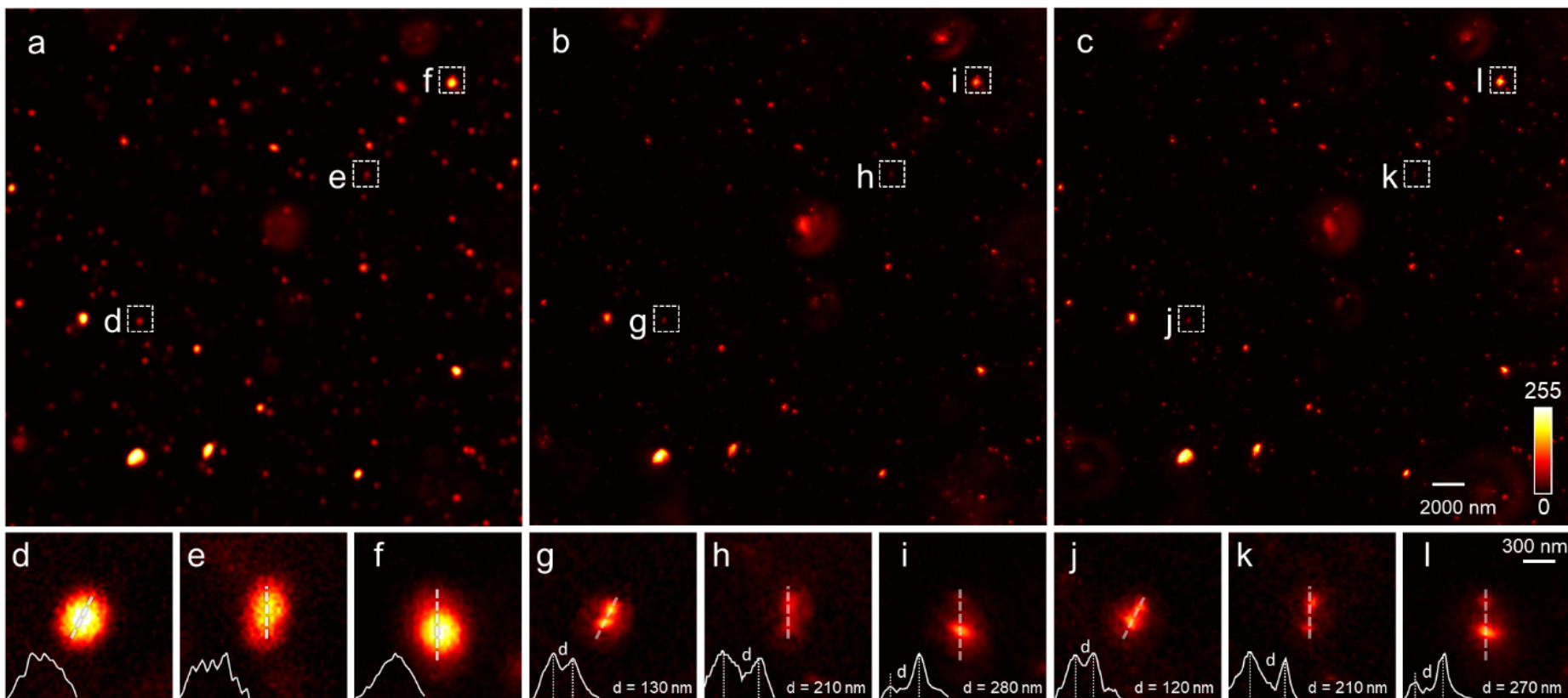


Quantification

Network input (100×/1.4NA, confocal)

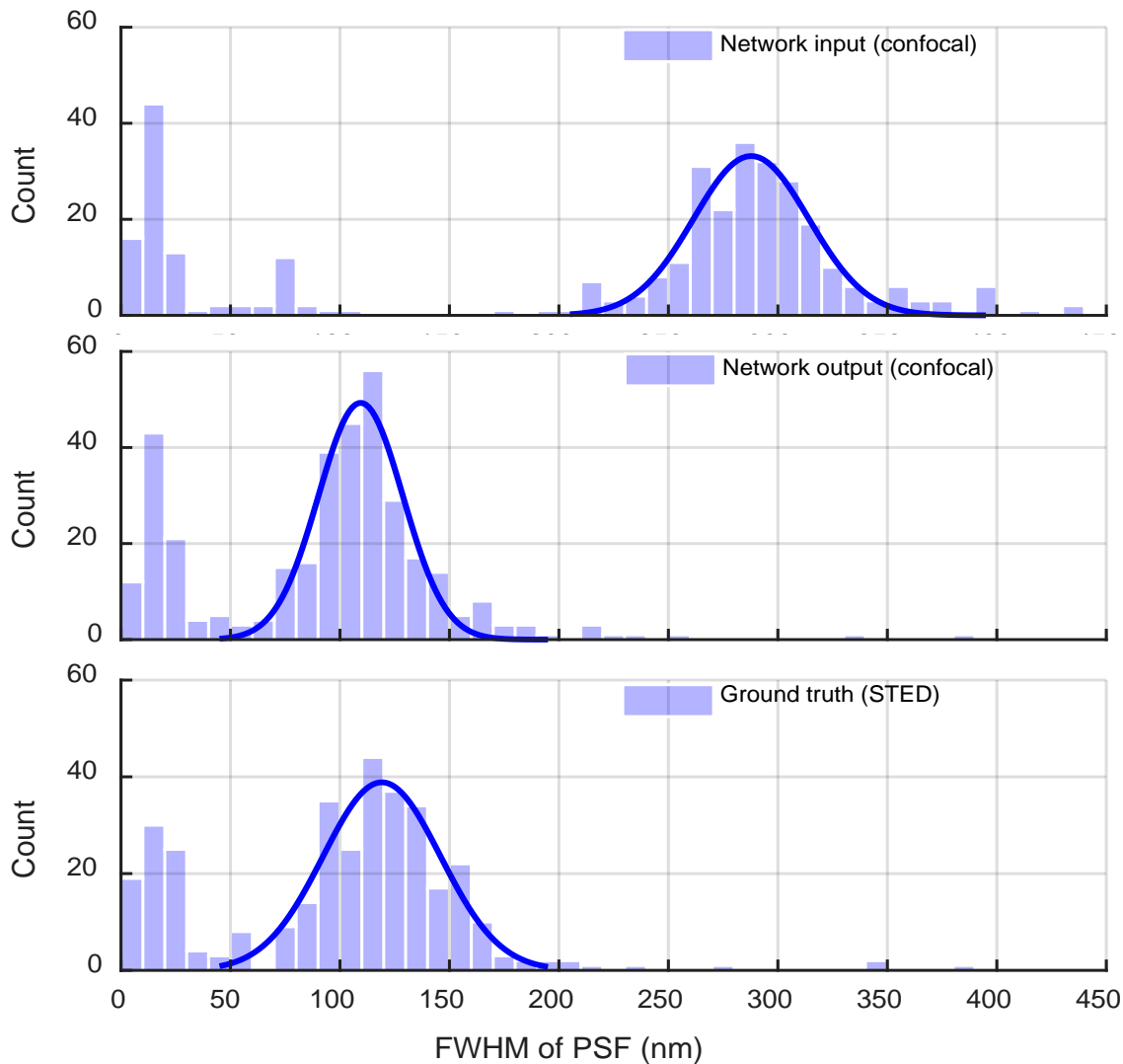
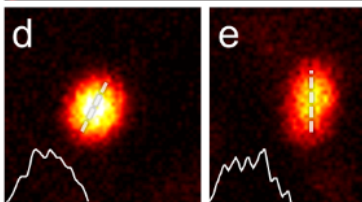
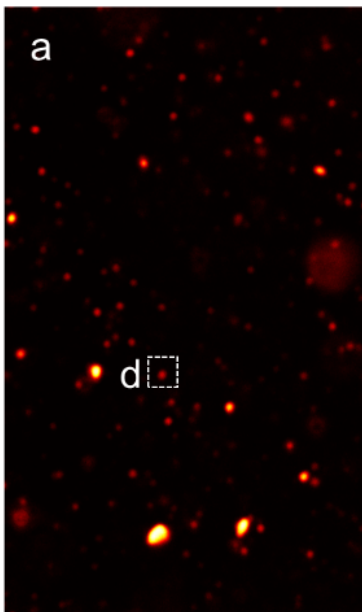
Network output (100×/1.4NA, confocal)

Ground truth (100×/1.4NA, STED)

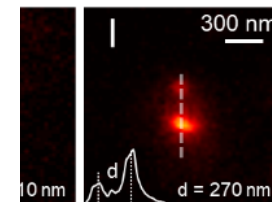
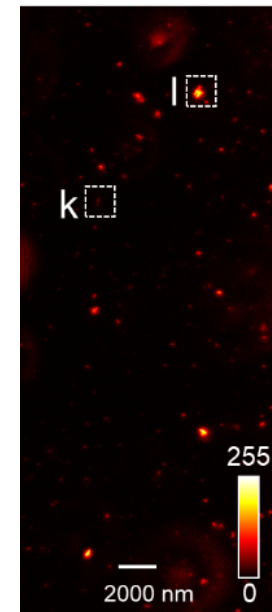


Quantification

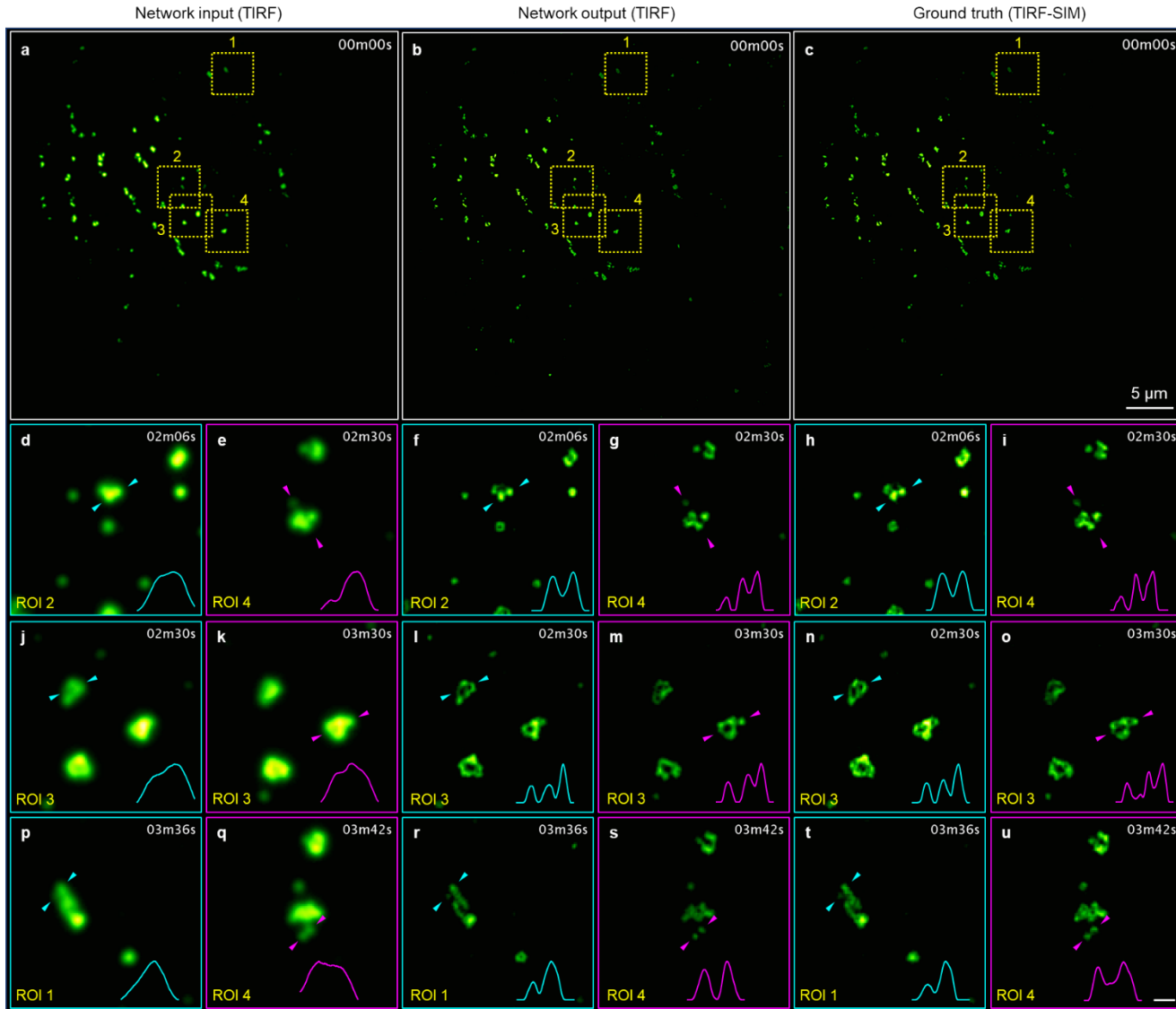
Network input (100×/1.



1.4NA, STED)



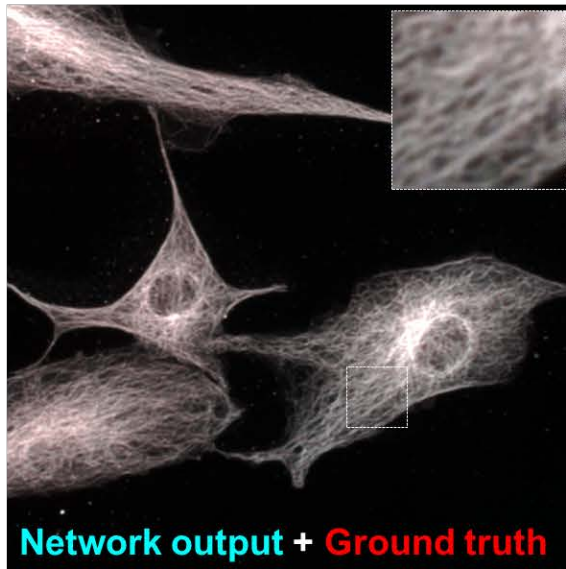
Imaging SUM159 cells expressing eGFP labeled clathrin adaptor AP2: TIRF \rightarrow TIRF-SIM imaging



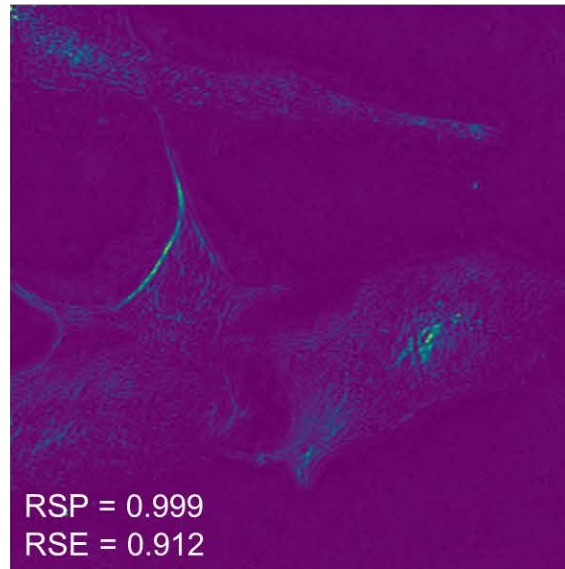
Error analysis with NanoJ-Squirrel toolbox¹

- Minimum differences was observed between the network output and the ground truth images.

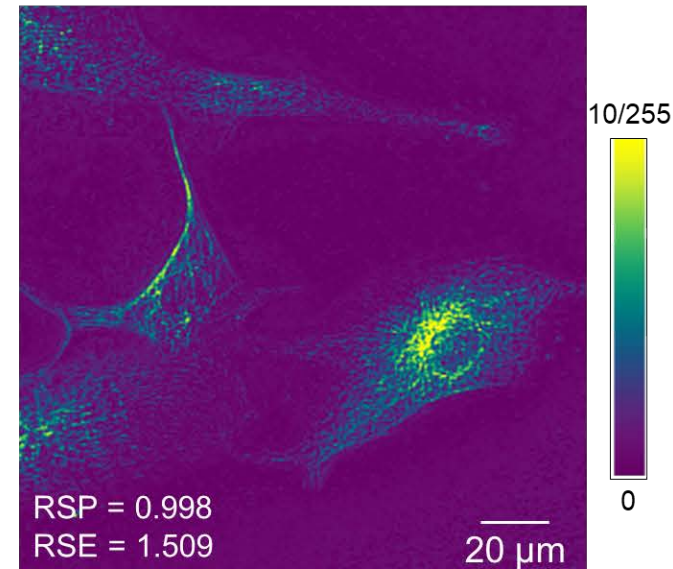
Overlay of output and ground truth



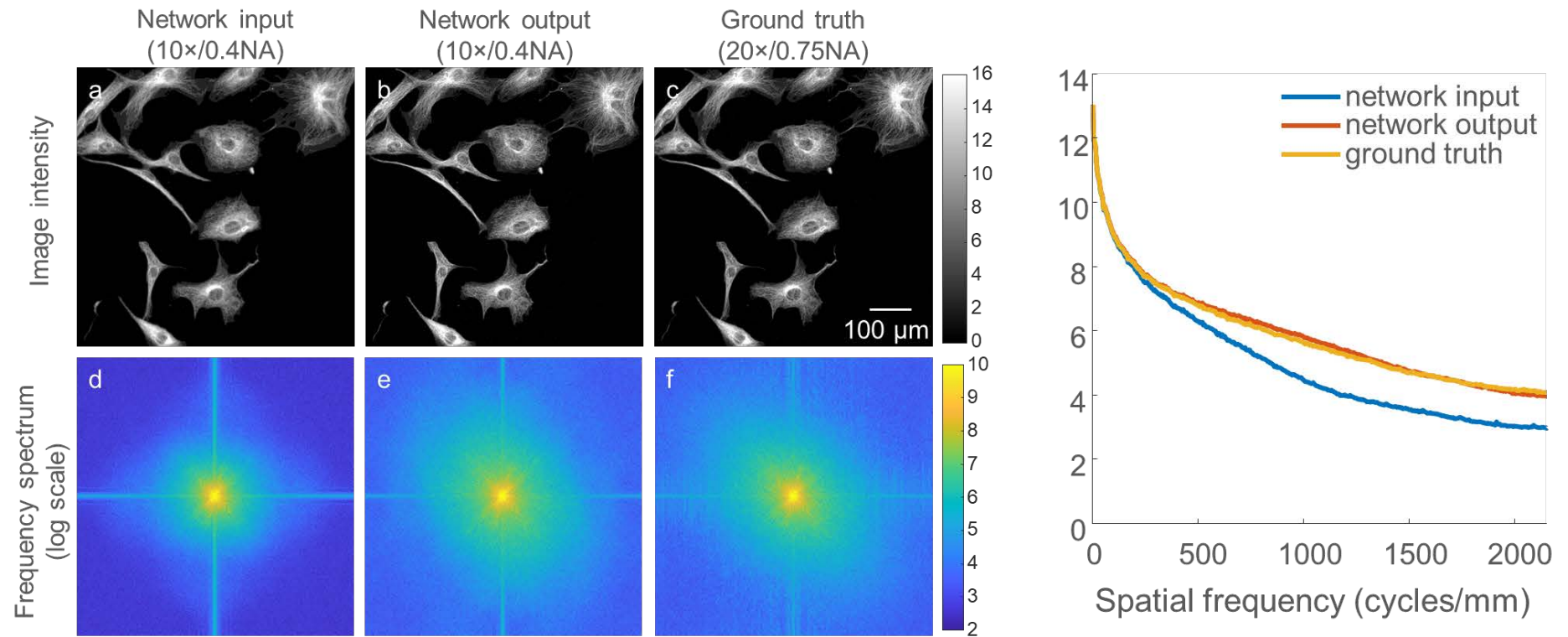
Error map (input vs. output)



Error map (input vs. ground truth)

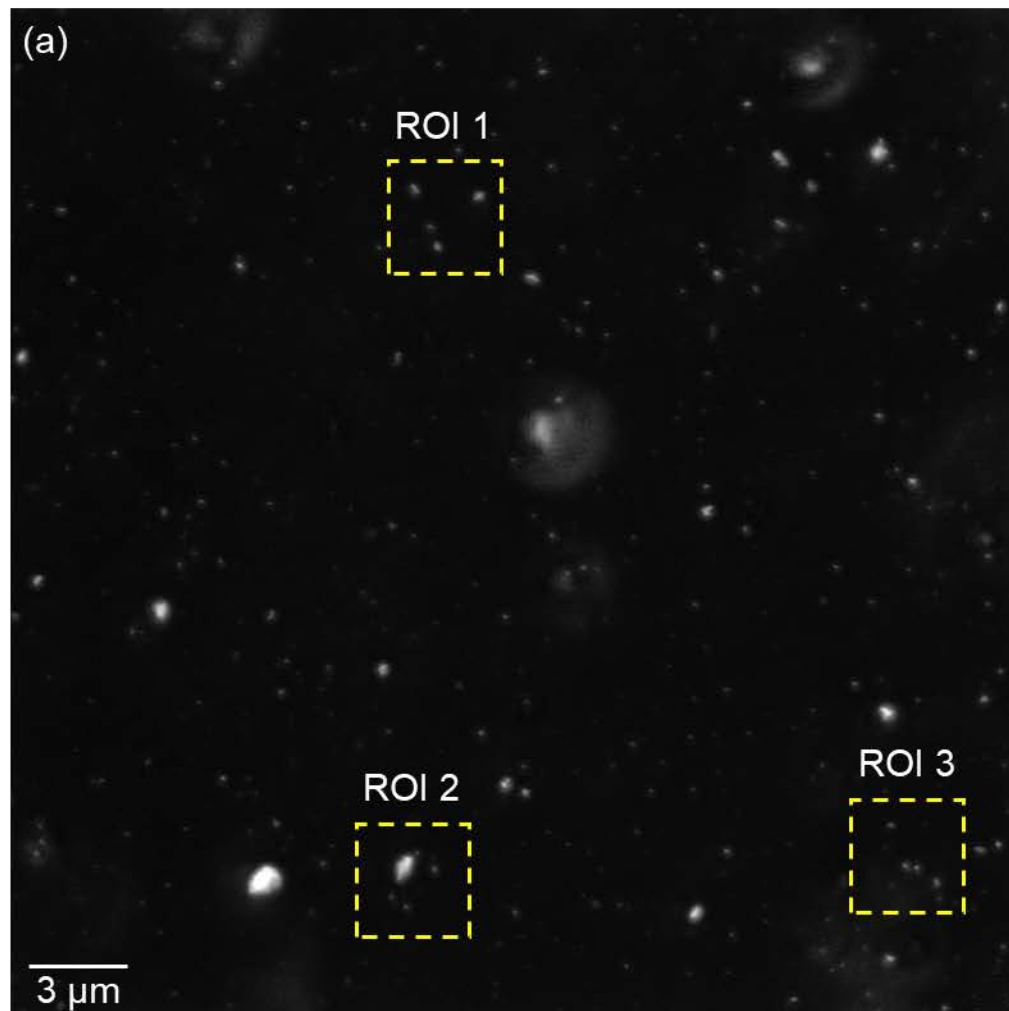


Spatial frequency spectrum analysis

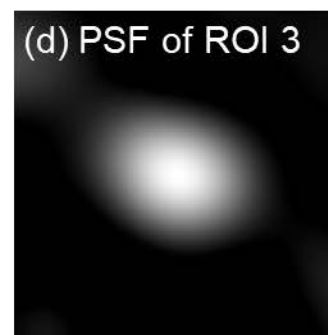
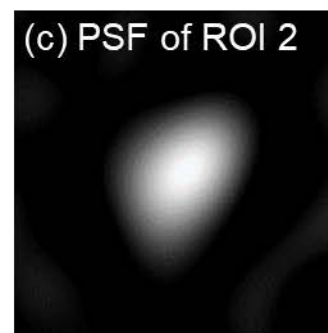
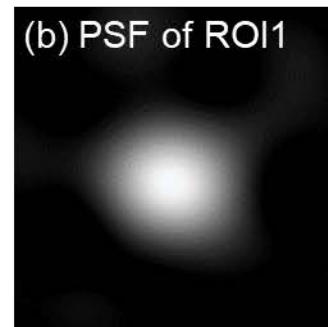


Spatially-varying PSFs measured by neural network

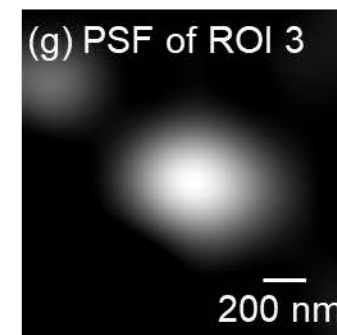
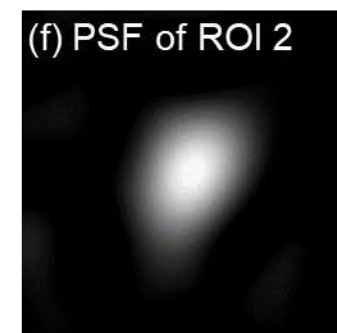
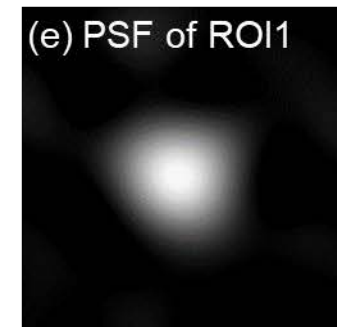
network output image (from confocal)



Deconvolved with network output

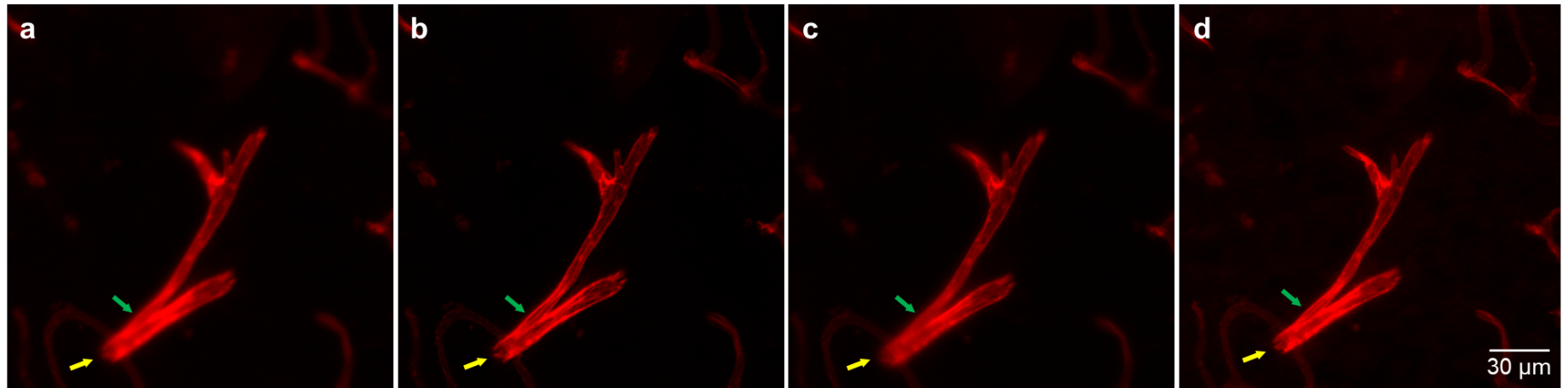


Deconvolved with ground truth



Network inferred image has extended depth-of-field

Network input (10×/0.4NA) Network output (10×/0.4NA) Ground truth (20×/0.75NA) EDOF image (20×/0.75NA)

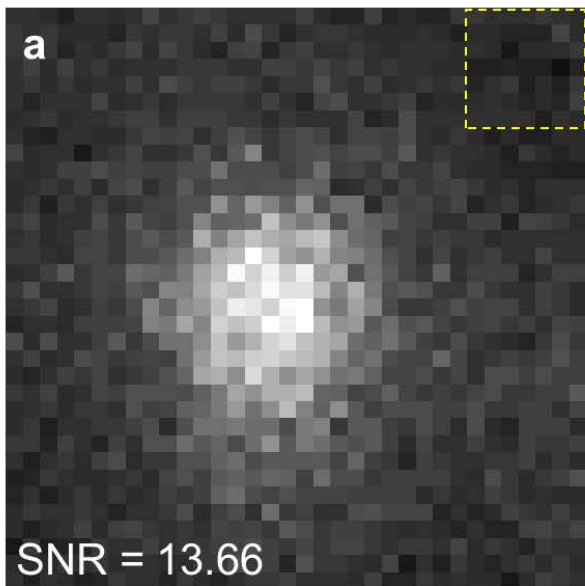


Synthesized from a z-stack of 34 images with 0.3 μm spacing

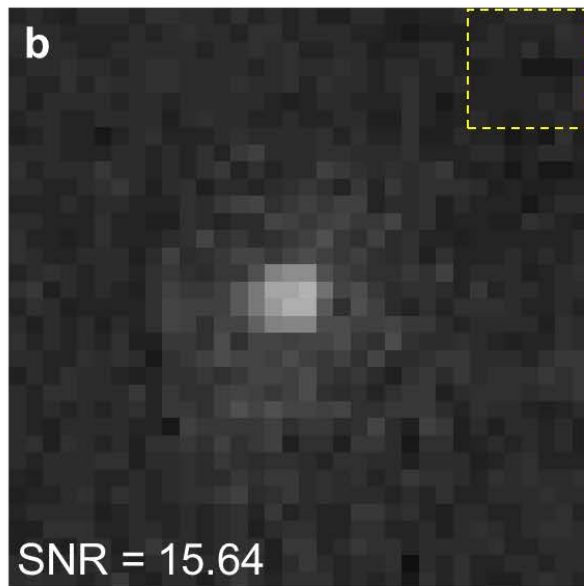
Green and **Yellow** arrows point to features that demonstrate **extended depth-of-focus** effect.

Network inferred image has higher SNR

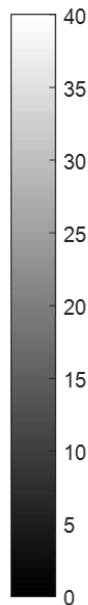
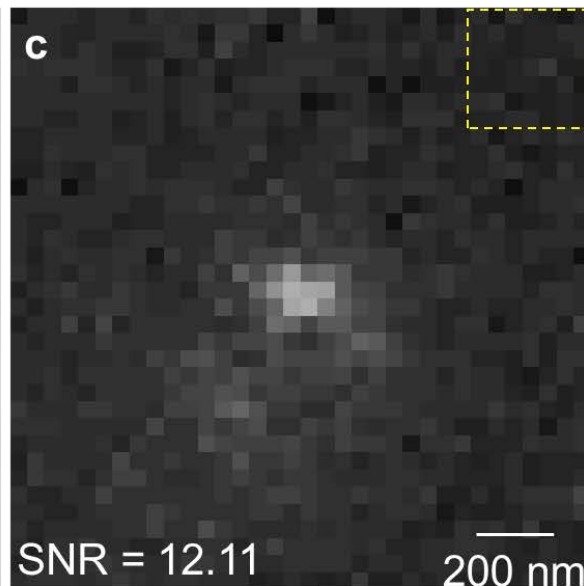
Network input (Confocal)



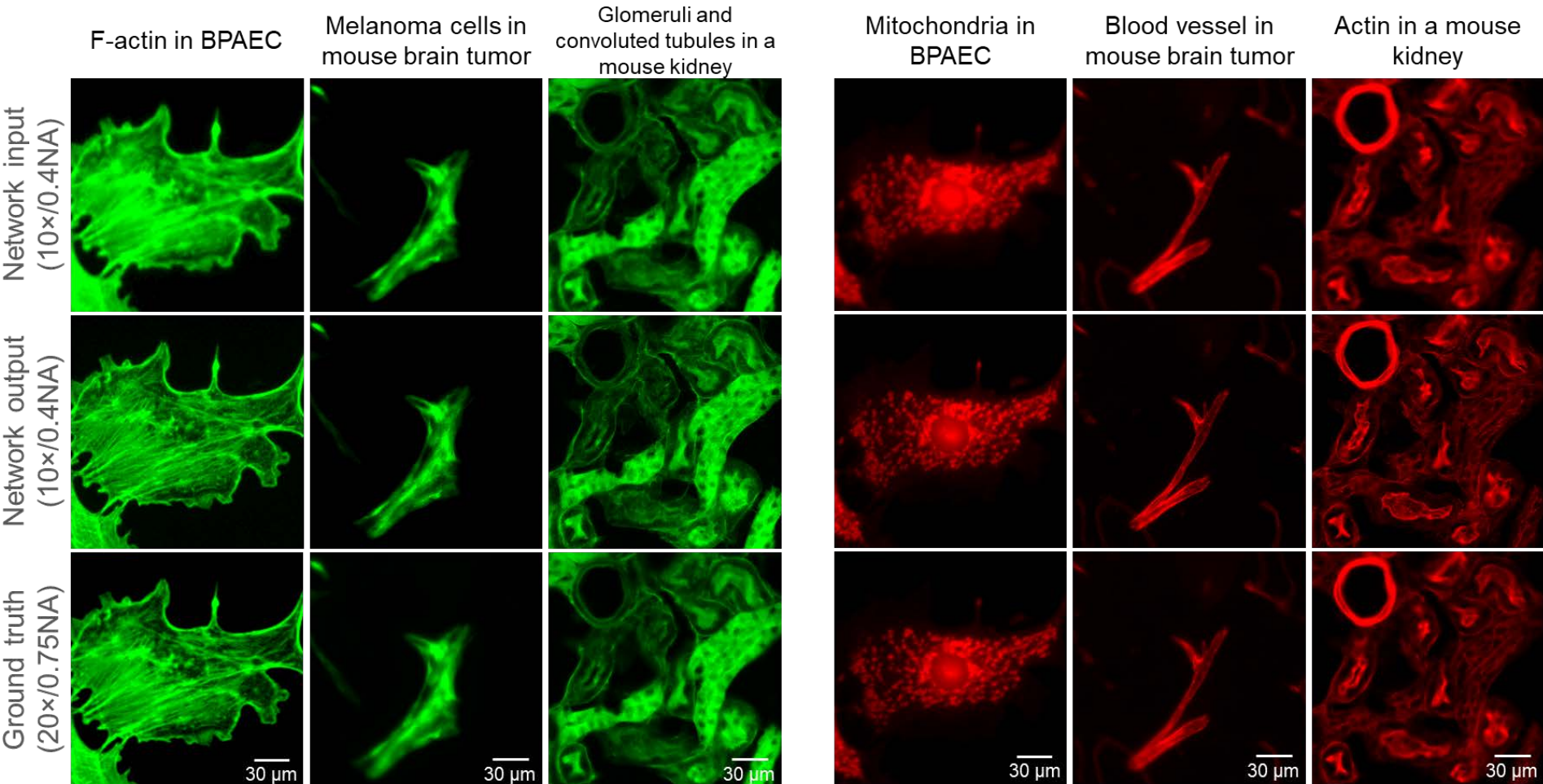
Network output (Confocal)



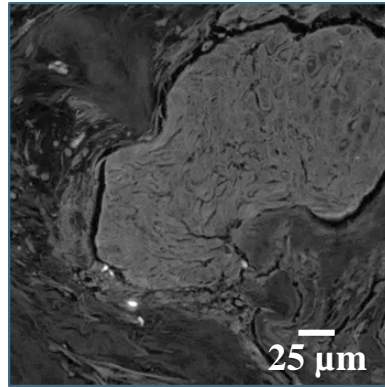
Ground truth (STED)



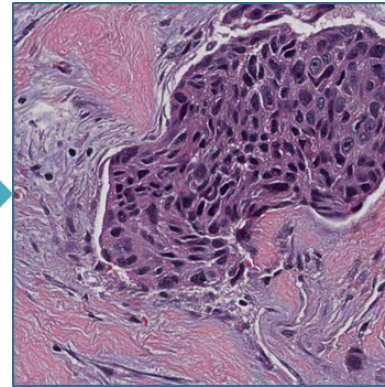
Generalization to new types of samples



Auto-fluorescence of
label free tissue section



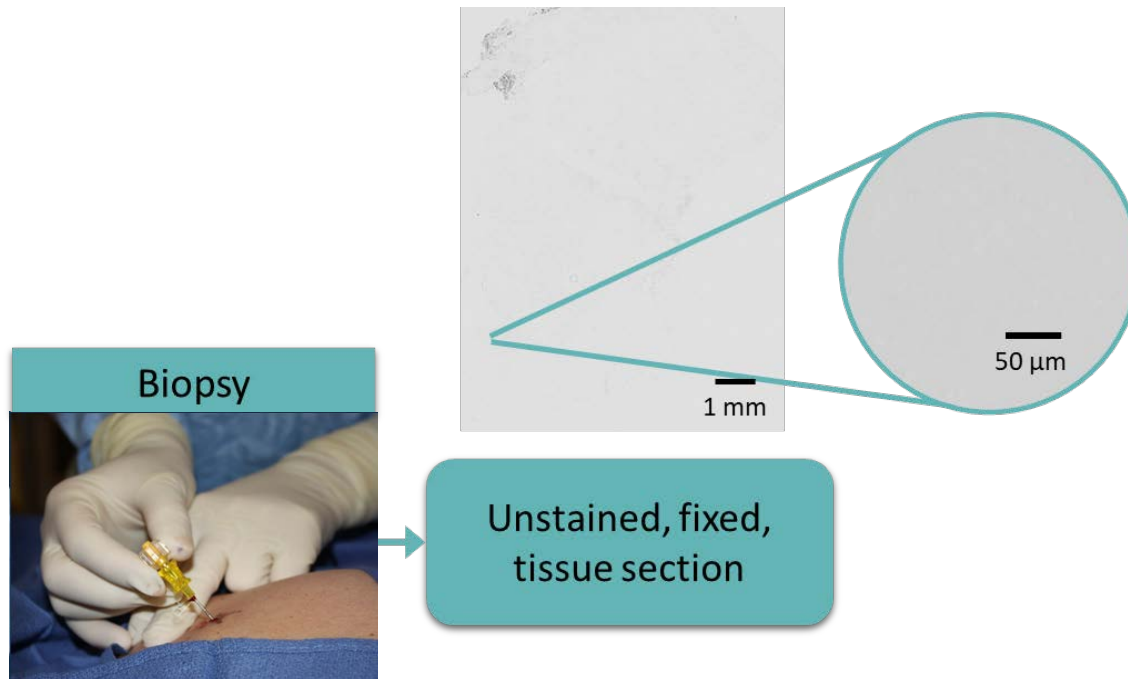
Virtual histochemical stain



DEEP LEARNING-BASED VIRTUAL HISTOLOGY STAINING USING AUTO- FLUORESCENCE OF LABEL-FREE TISSUE

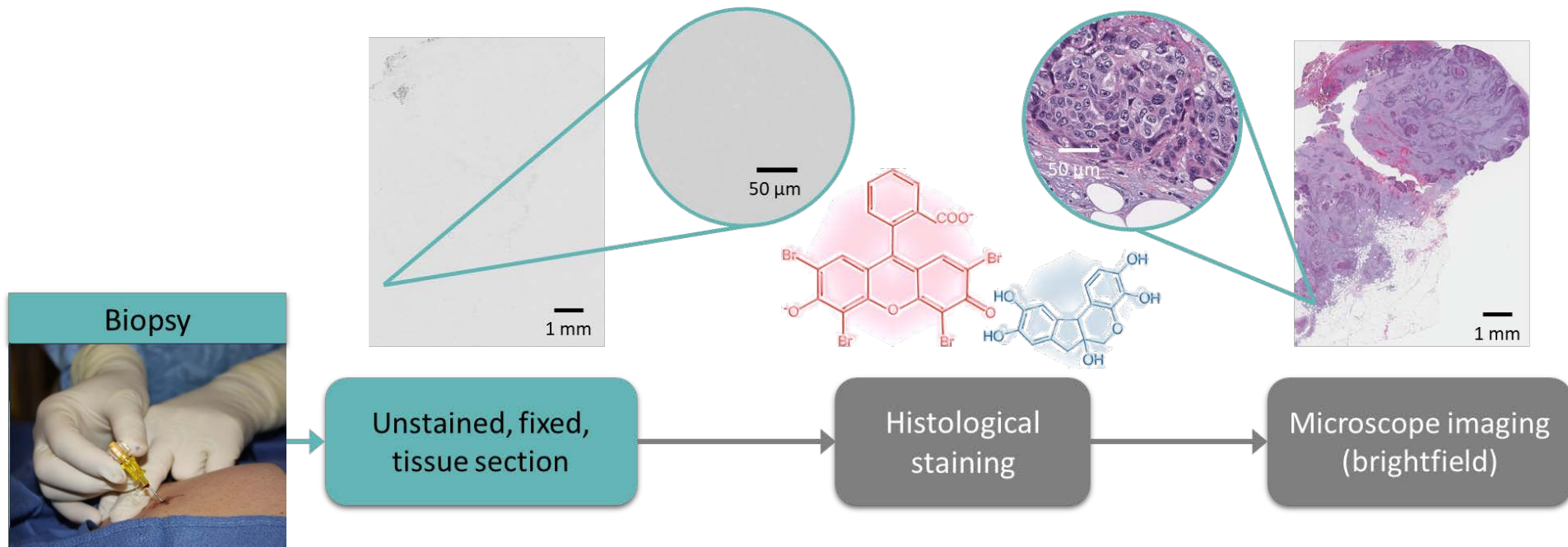
Histopathology

- Histopathology is the diagnosis and study of diseases of the tissues, and involves examining tissues and/or cells under a microscope.



Histological staining

- Histochemistry a technique that is used for the visualization of biological structures.



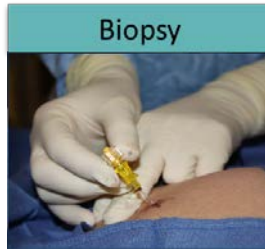
Histochemical staining drawbacks

- Laborious process
- Time consuming
- Expensive (reagents, training, personnel, monitoring)
- Doesn't support tissue preservation for advanced diagnosis
- Staining variation



<https://doi.org/10.1186/1746-1596-6-S1-S15>

Alternative contrasting methods



Tissue section (not necessarily thin)

Contrast inducing imaging

“Rapid” staining

Label free imaging

“Rapid” Staining:

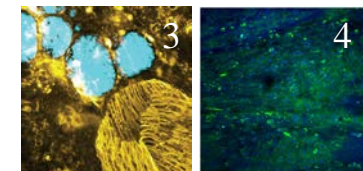
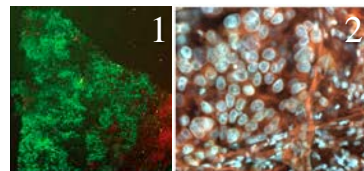
- Acridine orange
- Eosin

Imaging:

- 2PM
- SHG
- UV surface excitation

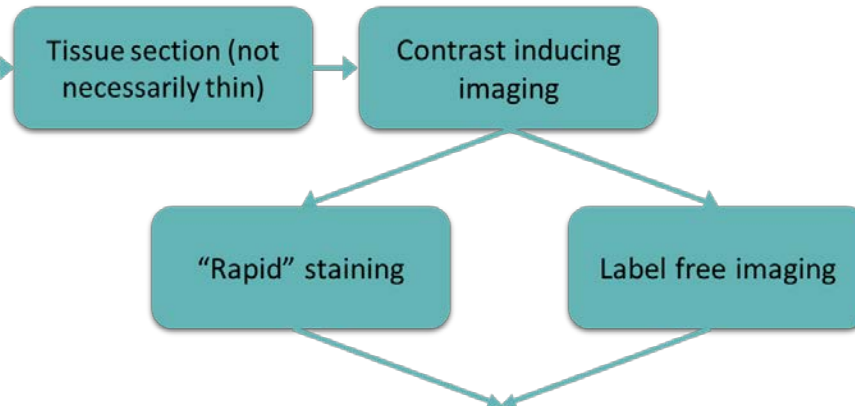
Label free Imaging:

- Autofluorescence – single photon, multi-photon
- HHG
- Stimulated Raman scattering microscopy
- Quantitative phase microscopy



1. Tao, Y. K. et al. Assessment of breast pathologies using nonlinear microscopy. *Proc. Natl. Acad. Sci.* 111, 15304–15309
2. Fereidouni, F. et al. Microscopy with ultraviolet surface excitation for rapid slide-free histology. *Nat. Biomed. Eng.* 1, 957–966 (2017).
3. Tu, H. et al. Stain-free histopathology by programmable supercontinuum pulses. *Nat. Photonics* 10, 534–540 (2016).
4. Orringer, D. A. et al. Rapid intraoperative histology of unprocessed surgical specimens via fibre-laser-based stimulated Raman scattering microscopy. *Nat. Biomed. Eng.* 1, 0027 (2017).

Interpretability



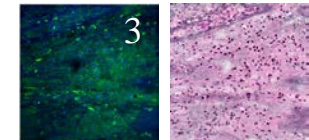
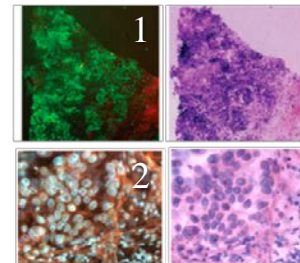
Training:

- Experts
- Algorithms

- Costly
- Lack of data

Pseudo-staining

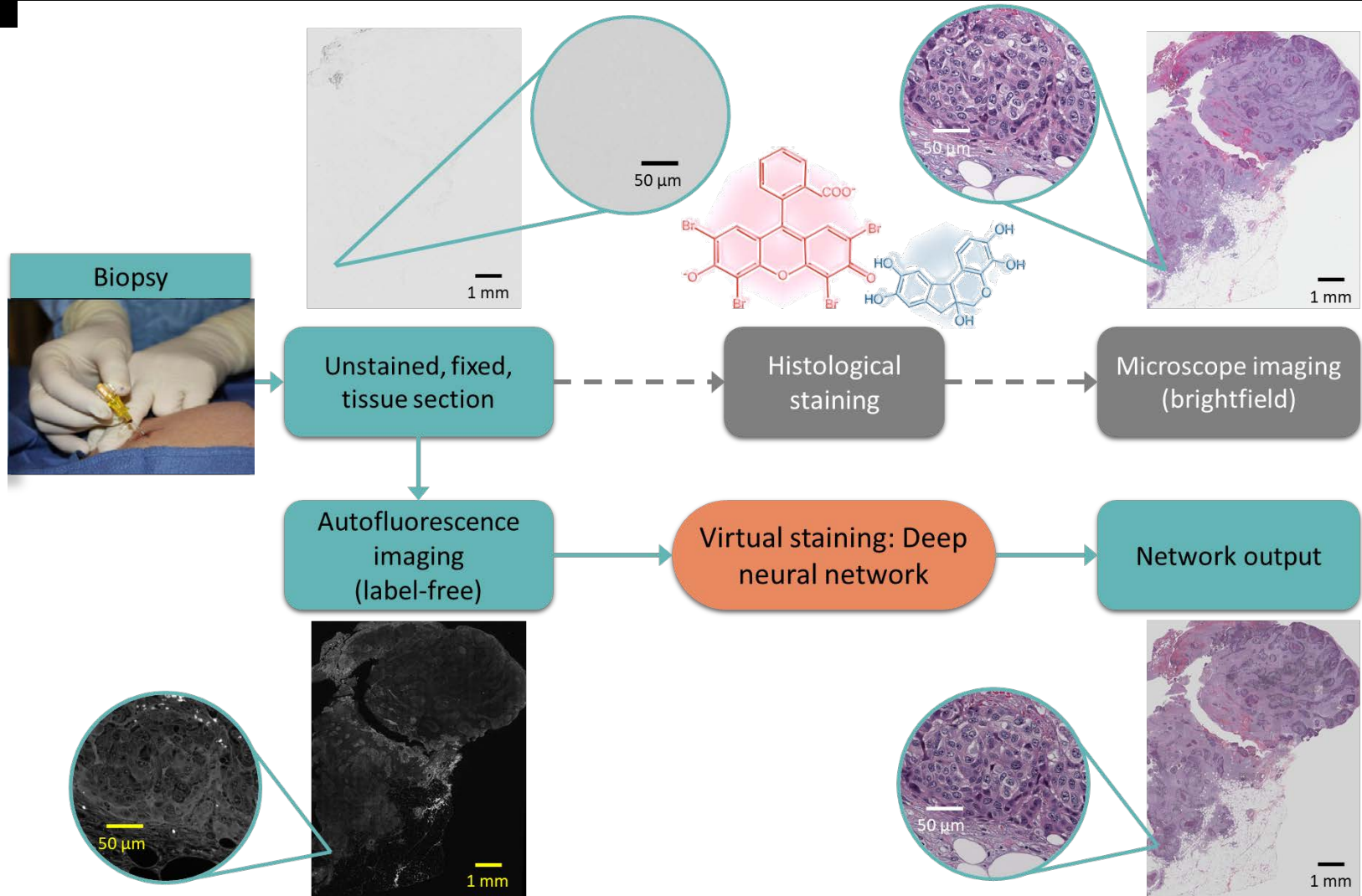
Based on approximation of the intensity as a function of the dye concentration



Requires multiple images / spectra / rapid staining

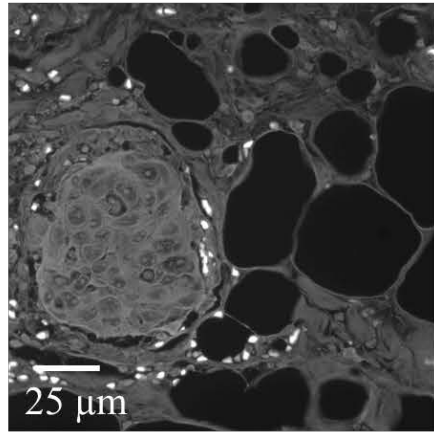
1. Tao, Y. K. et al. Assessment of breast pathologies using nonlinear microscopy. Proc. Natl. Acad. Sci. 111, 15304–15309
2. Fereidouni, F. et al. Microscopy with ultraviolet surface excitation for rapid slide-free histology. Nat. Biomed. Eng. 1, 957–966 (2017).
3. Orringer, D. A. et al. Rapid intraoperative histology of unprocessed surgical specimens via fibre-laser-based stimulated Raman scattering microscopy. Nat. Biomed. Eng. 1, 0027 (2017).

Deep learning-based virtual staining using auto-fluorescence of label-free tissue

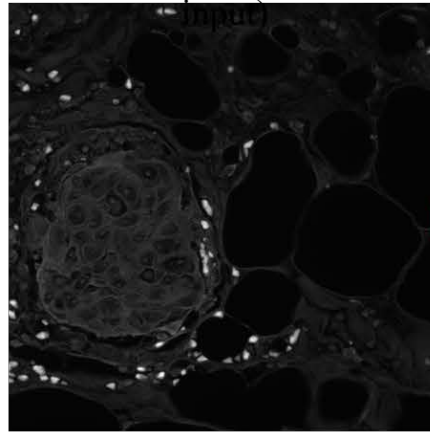


Virtual H&E staining (Salivary gland tissue)

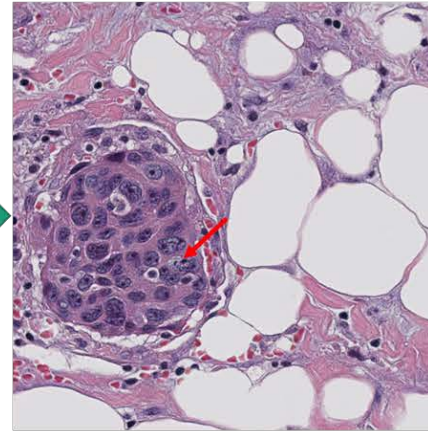
Contrast enhanced unstained tissue DAPI image



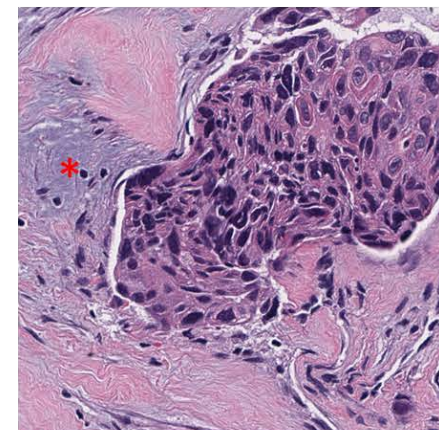
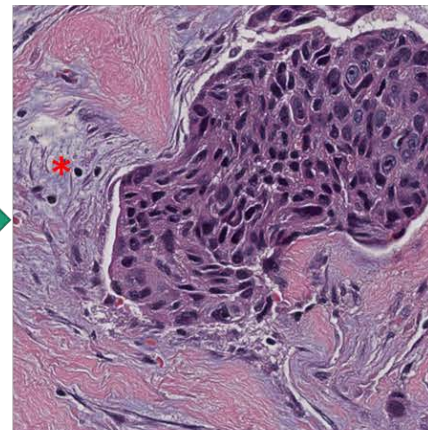
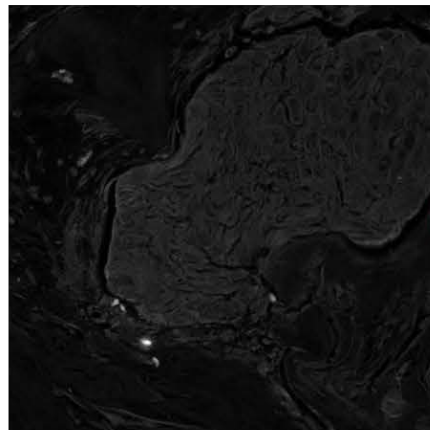
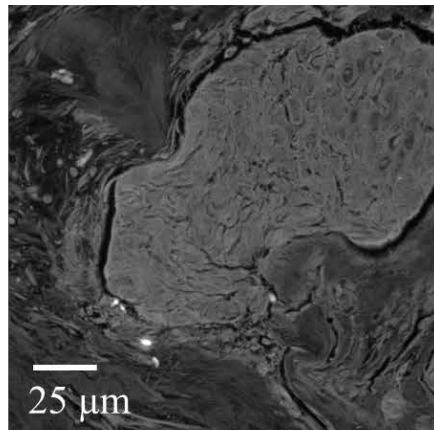
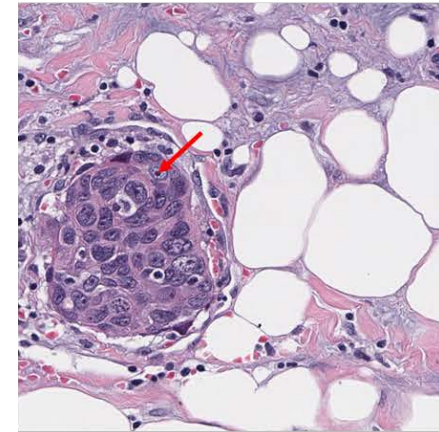
Unstained salivary gland tissue DAPI image (network input)



H&E *virtually* stained salivary gland tissue (network output)

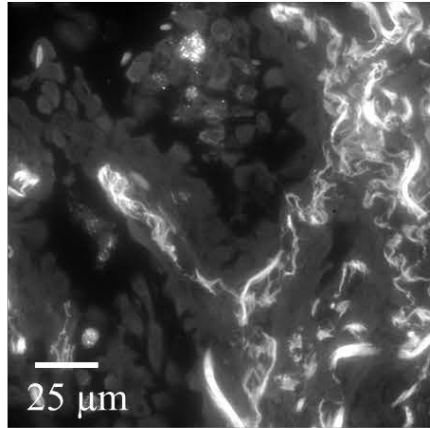


H&E *historically* stained salivary gland tissue

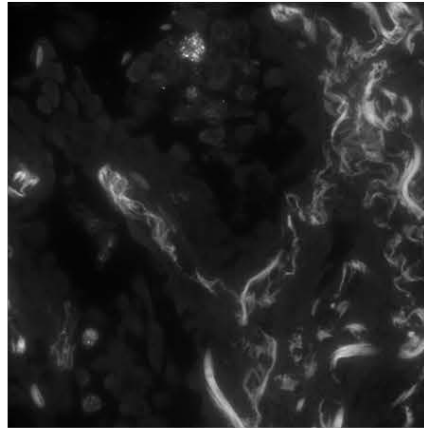


Virtual Masson's Trichrome staining (lung tissue)

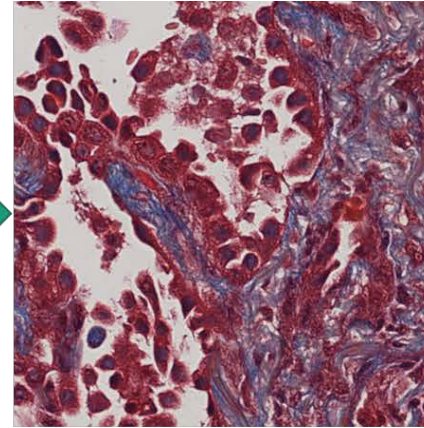
Contrast enhanced unstained tissue auto-fluorescent image



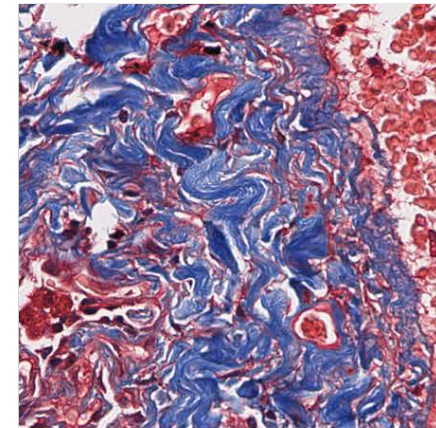
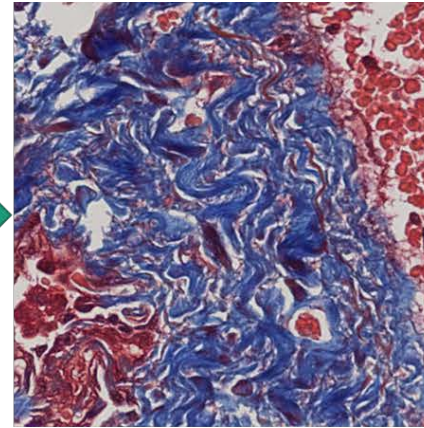
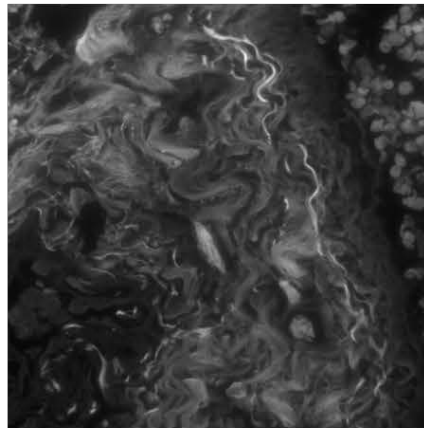
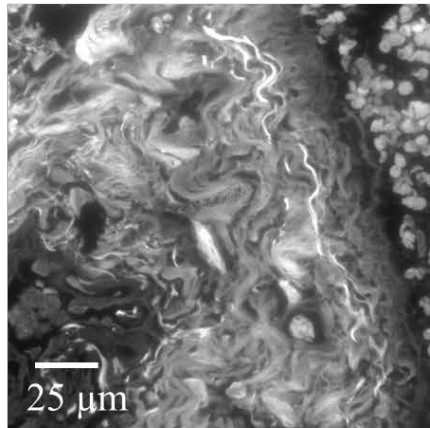
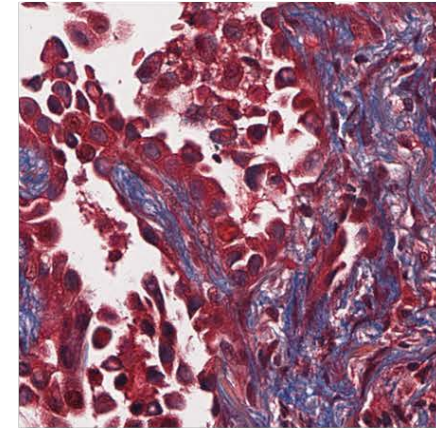
Unstained tissue auto-fluorescent image



MT3 *virtually* stained tissue (network output)

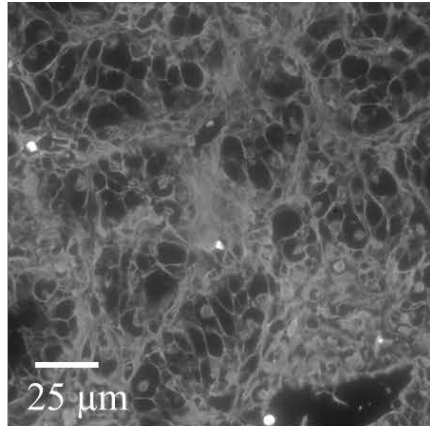


MT3 *chemically* stained tissue (brightfield)

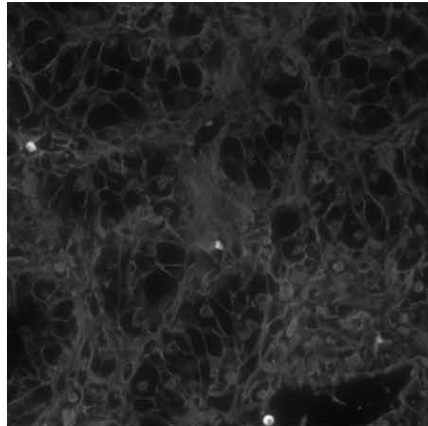


Virtual Jones' silver staining (kidney tissue)

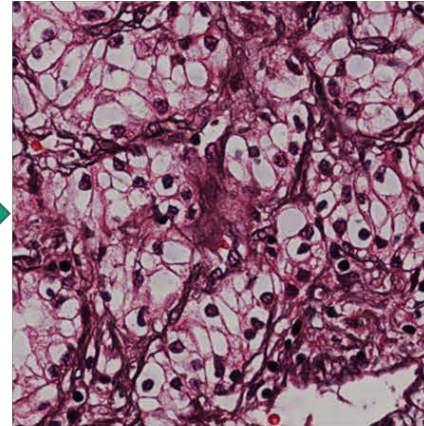
Contrast enhanced unstained tissue DAPI image



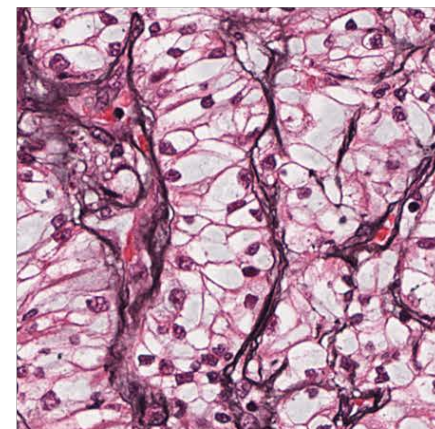
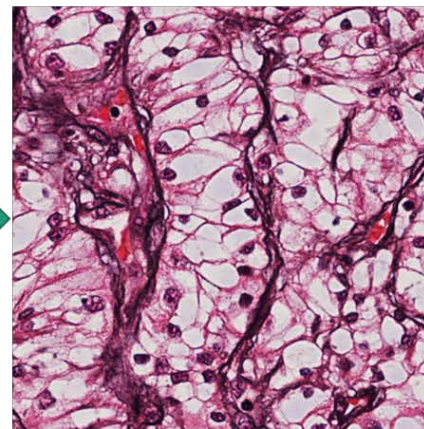
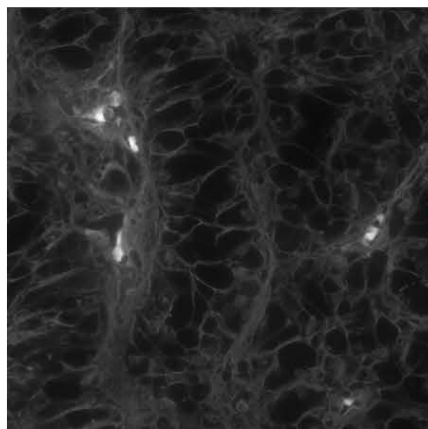
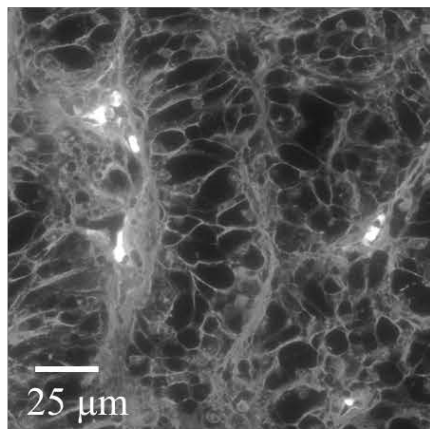
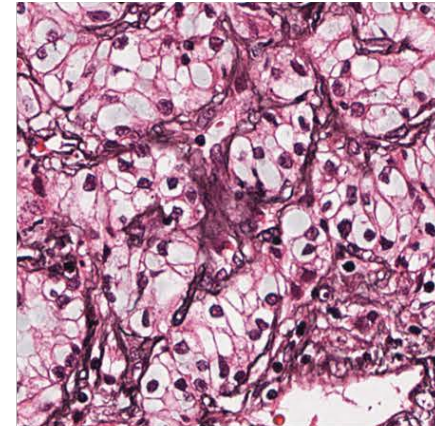
Unstained tissue DAPI image (network input)



H&E *virtually* stained tissue (network output)



Jones Silver stained tissue



Blind assessment by pathologists

Serial number	Tissue, fixation, stain	Pathologist #	Histochemically / Virtually stained	Diagnosis
1	Ovary, Frozen section, H&E	1	VS	Adenocarcinoma
		2	VS	Borderline serous tumor
		3	HS	Mucinous adenocarcinoma
		4	HS	Adenocarcinoma, endometrioid
2	Ovary, Frozen section, H&E	1	VS	Benign ovary
		2	VS	Benign ovary
		3	HS	Normal ovary with corpus luteal cyst
		4	HS	Normal
3	Salivary Gland, FFPE, H&E	1	VS	Benign salivary glands with mild chronic inflammation
		2	VS	Benign parotid tissue
		3	HS	Normal salivary gland
		4	HS	No histopathologic abnormality
8	Prostate, FFPE, H&E	1	HS	Prostatic adenocarcinoma 3+4
		2	HS	Prostatic adenocarcinoma 4+3
		3	VS	Prostatic adenocarcinoma, Gleason pattern 3+4
		4	VS	HG-PIN with cribriforming vs carcinoma
15	Thyroid, FFPE, H&E	1	VS	Papillary thyroid carcinoma
		2	VS	Papillary thyroid ca
		3	HS	Papillary thyroid carcinoma
		4	HS	PTC

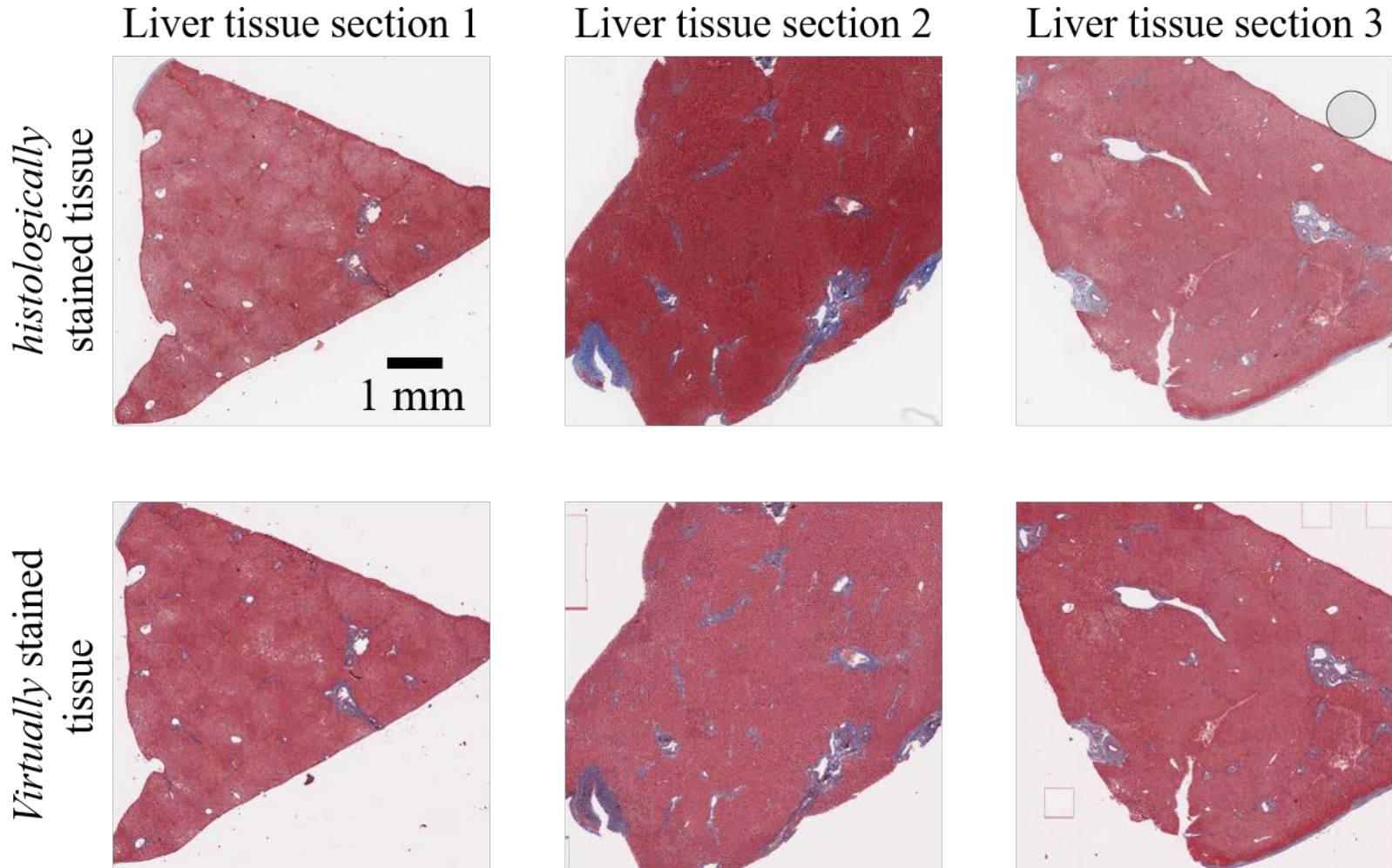
- The analysis of 15 tissue section images by 4 board certified pathologists (who weren't aware of the virtual staining technique) demonstrates 100% non-major discordance, defined as no clinically significant difference in diagnosis between observers.

Stain quality assessment by pathologists

Tissue #	Pathologist 1				Pathologist 2				Pathologist 3				Average			
	ND	CD	EF	SQ	ND	CD	EF	SQ	ND	CD	EF	SQ	ND	CD	EF	SQ
1 – HS	3	2	1	1	4	4	3	4	1	1	1	3	2.67	2.33	1.67	2.67
1 - VS	3	3	3	3	3	3	2	3	2	2	3	3	2.67	2.67	2.67	3.00
2 – HS	3	2	4	4	4	4	3	4	1	2	2	2	2.67	2.67	3.00	3.33
2 - VS	3	3	4	4	4	3	3	3	2	2	3	3	3.00	2.67	3.33	3.33
3 – HS	3	3	2	2	3	3	4	3	1	1	1	1	2.33	2.33	2.33	2.00
3 - VS	3	2	1	1	3	3	1	4	1	1	1	1	2.33	2.00	1.00	2.00
4 – HS	3	2	4	4	3	4	4	4	1	2	1	2	2.33	2.67	3.00	3.33
4 - VS	3	3	4	4	4	3	4	4	2	2	3	3	3.00	2.67	3.67	3.67
5 – HS	3	3	4	4	3	3	2	1	1	3	2	2	2.33	3.00	2.67	2.33
5 - VS	3	2	3	3	3	3	4	2	2	1	3	3	2.67	2.00	3.33	2.67
6 – HS	3	2	3	3	4	4	4	3	2	2	2	2	3.00	2.67	3.00	2.67
6 - VS	3	3	4	3	4	3	4	3	1	1	1	1	2.67	2.33	3.00	2.33
7 – HS	3	3	4	4	3	4	4	3	2	1	2	2	2.67	2.67	3.33	3.00
7 - VS	3	2	3	3	4	4	4	3	2	2	3	3	3.00	2.67	3.33	3.00
8 – HS	3	3	4	4	4	4	4	3	1	1	1	1	2.67	2.67	3.00	2.67
8 - VS	3	2	4	4	4	3	4	4	2	2	3	2	3.00	2.33	3.67	3.33

nuclear detail (ND), cytoplasmic detail (CD) and extracellular fibrosis (EF) and overall stain (SQ) ;
 4 = perfect, 3 = very good, 2 = acceptable, 1 = unacceptable

Staining standardization





DEEP LEARNING BASED HOLOGRAPHIC IMAGE RECONSTRUCTION AND PHASE RECOVERY

Rivenson, Y. *, Zhang, Y. *, Gunaydin, H., Teng, D. & Ozcan, A. Phase recovery and holographic image reconstruction using deep learning in neural networks. *Light Sci. Appl.* 7, e17141

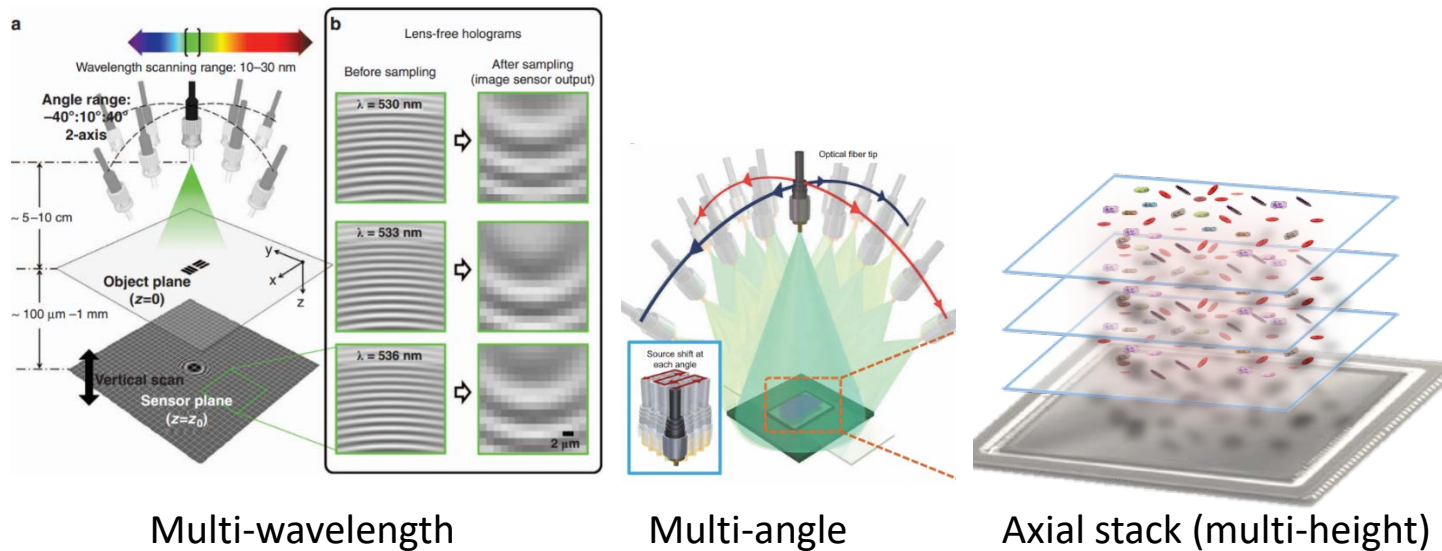
Coherent imaging systems

- Coherent illumination interaction with a specimen:

$$A_{out}(x, y) = A_0 a(x, y) e^{-j\phi(x, y)}$$

- The propagated wave complex field amplitude allows us to capture all the information about the specimen.
- Optoelectronic sensors are only sensitive to the intensity of light, i.e, phase information cannot be directly acquired.

Phase retrieval via measurement diversity



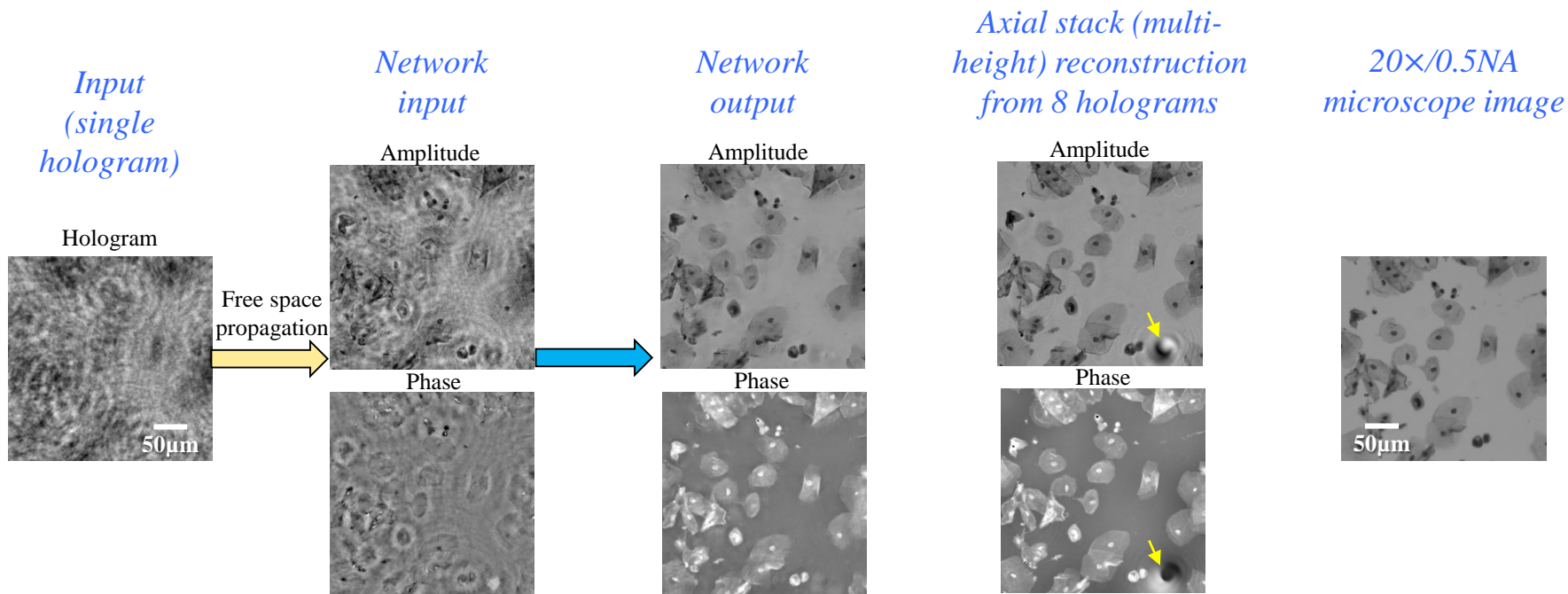
W. Luo, Y. Zhang, A. Feizi, Z. Gorocs, and A. Ozcan, "Pixel super-resolution using wavelength scanning," *Light: Science & Applications* (Nature Publishing Group) (2015)

W. Luo, A. Greenbaum, Y. Zhang, and A. Ozcan, "Synthetic aperture based on-chip microscopy," *Light: Science & Applications* (Nature Publishing Group) (2015)

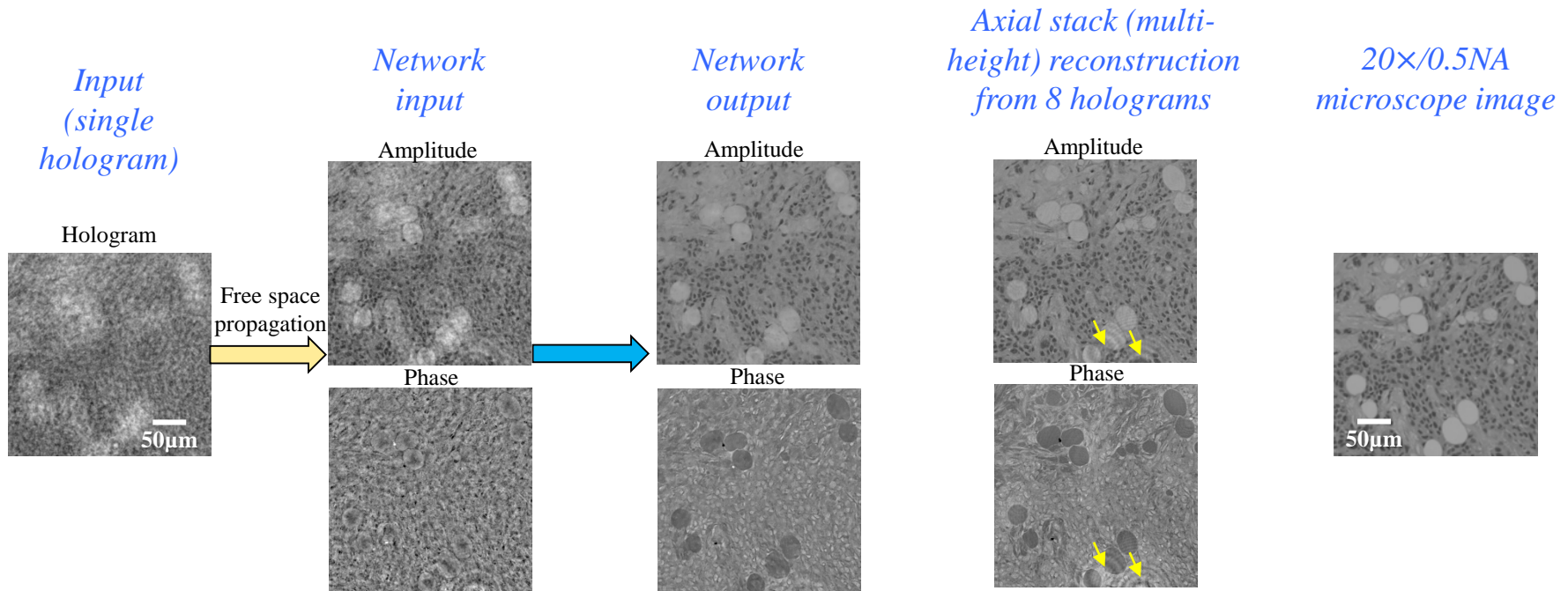
A. Greenbaum, et al, "Wide-field Computational Imaging of Pathology Slides using Lensfree On-Chip Microscopy," *Science Translational Medicine* (AAAS) (2014)

And many others...

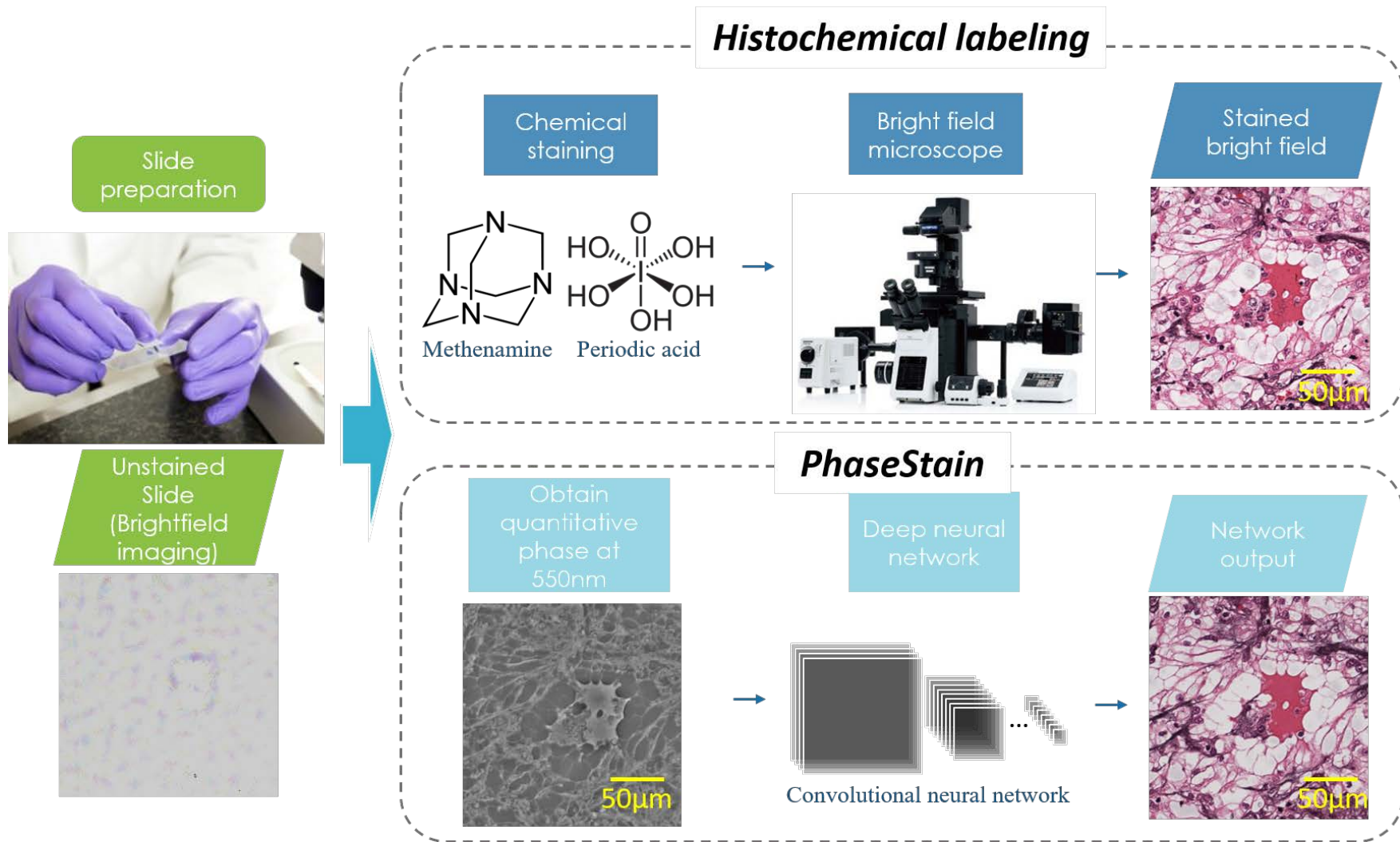
Inference results – on chip holographic microscopy (Papanicolaou smear)



Inference results – on chip holographic microscopy (Breast tissue section)

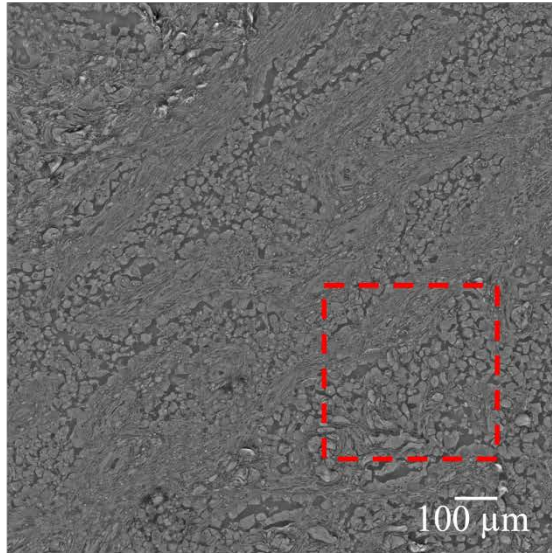


Virtual staining through specimen optical path length

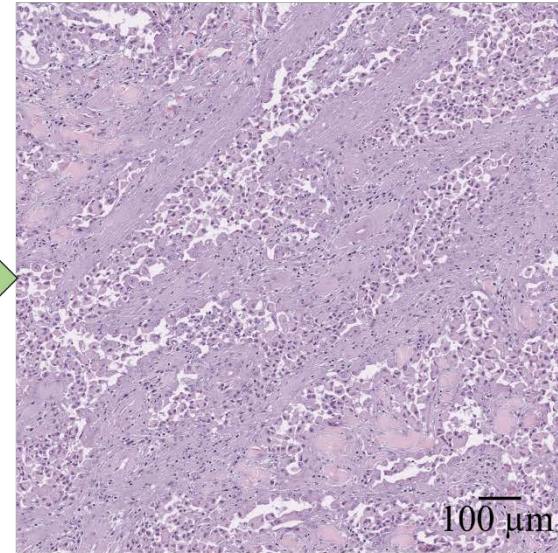


Virtual staining through specimen optical path length

QPI of label-free skin tissue section



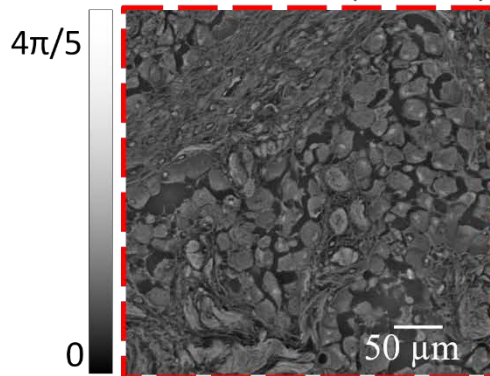
Network output –digital H&E staining



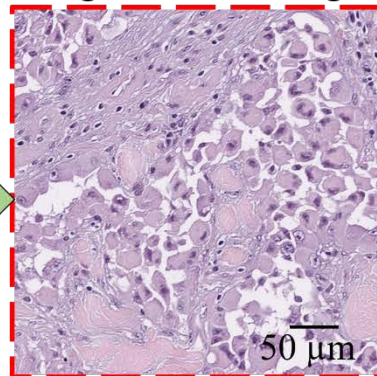
Trained
Network



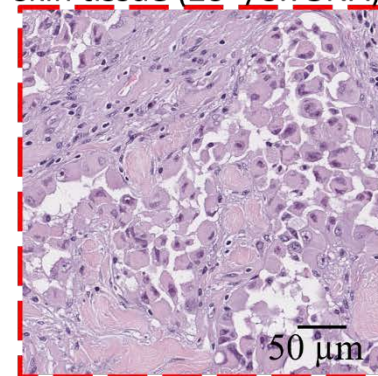
QPI of label-free skin tissue section (zoom in)



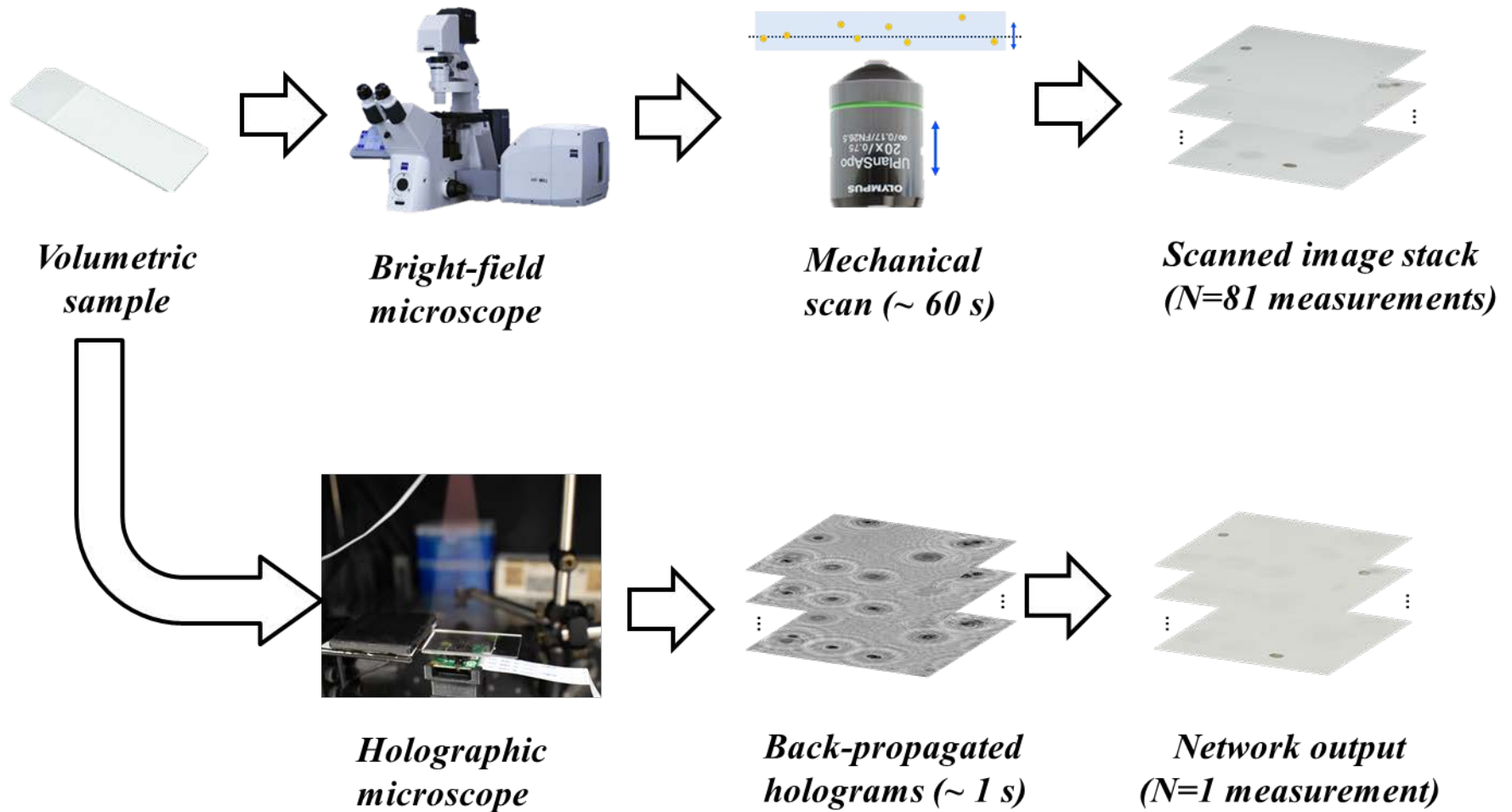
Network output – digital H&E staining



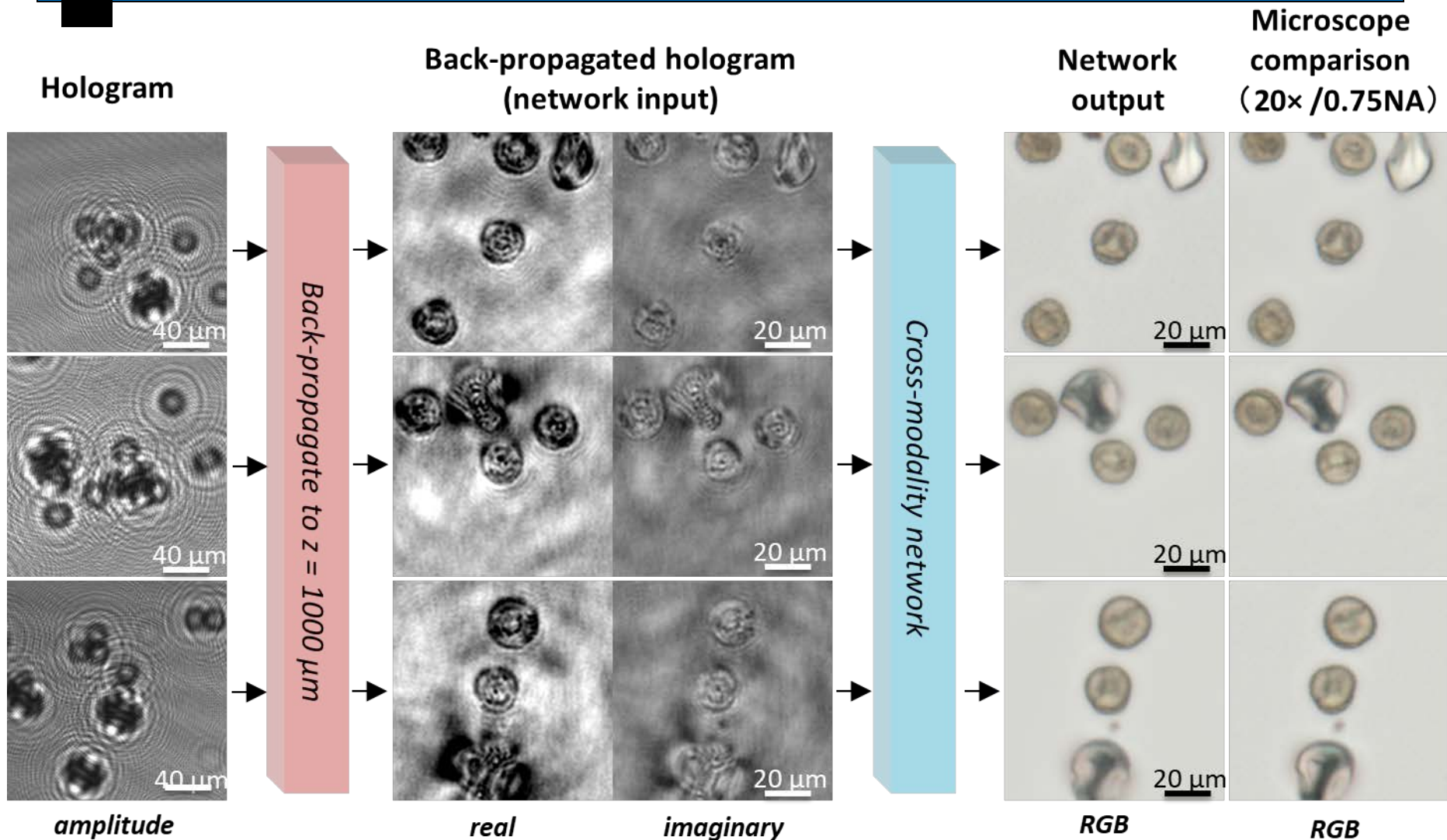
Brightfield image of the H&E chemically stained skin tissue (20×/0.75NA)



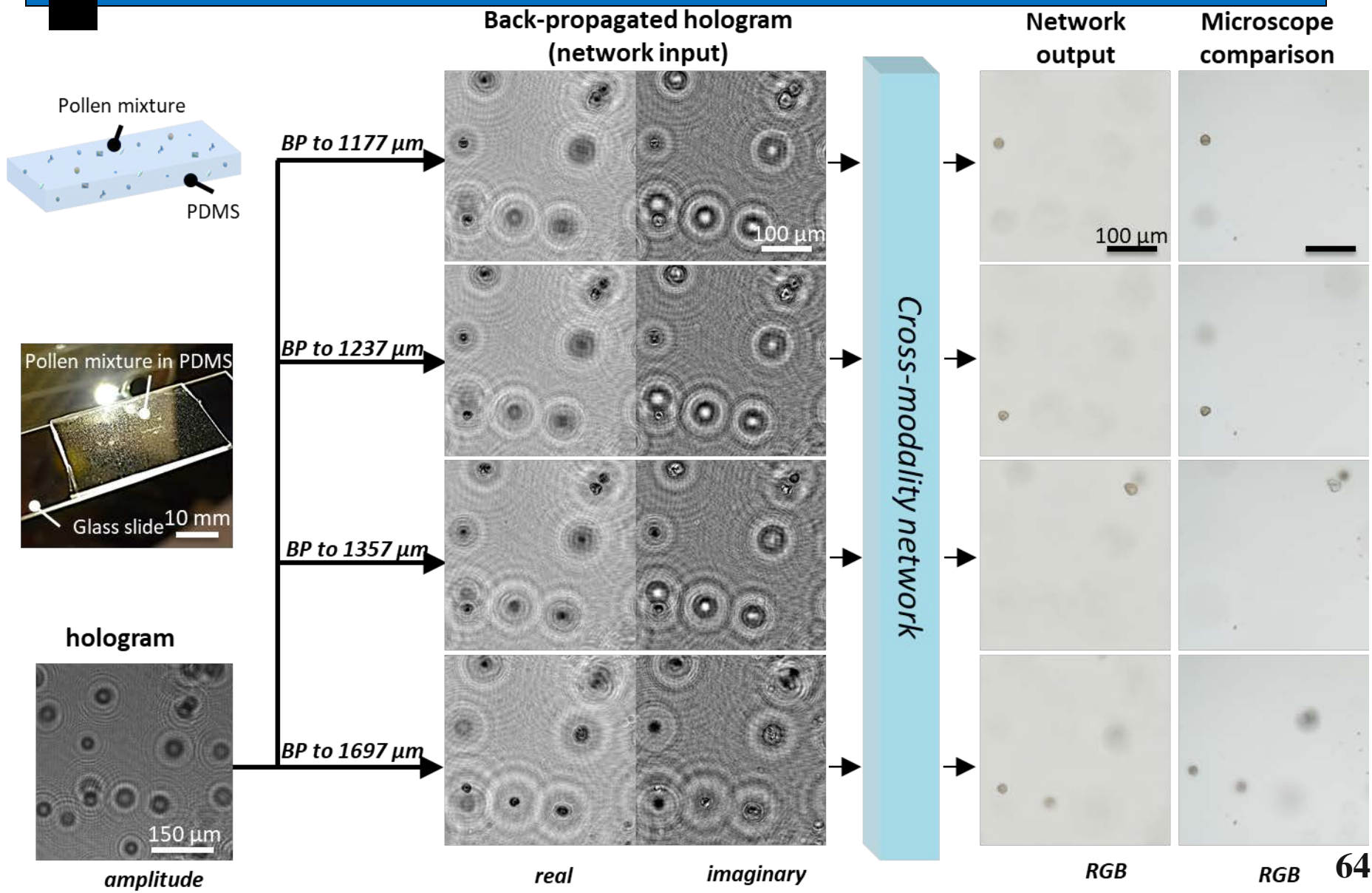
Brightfield Holography



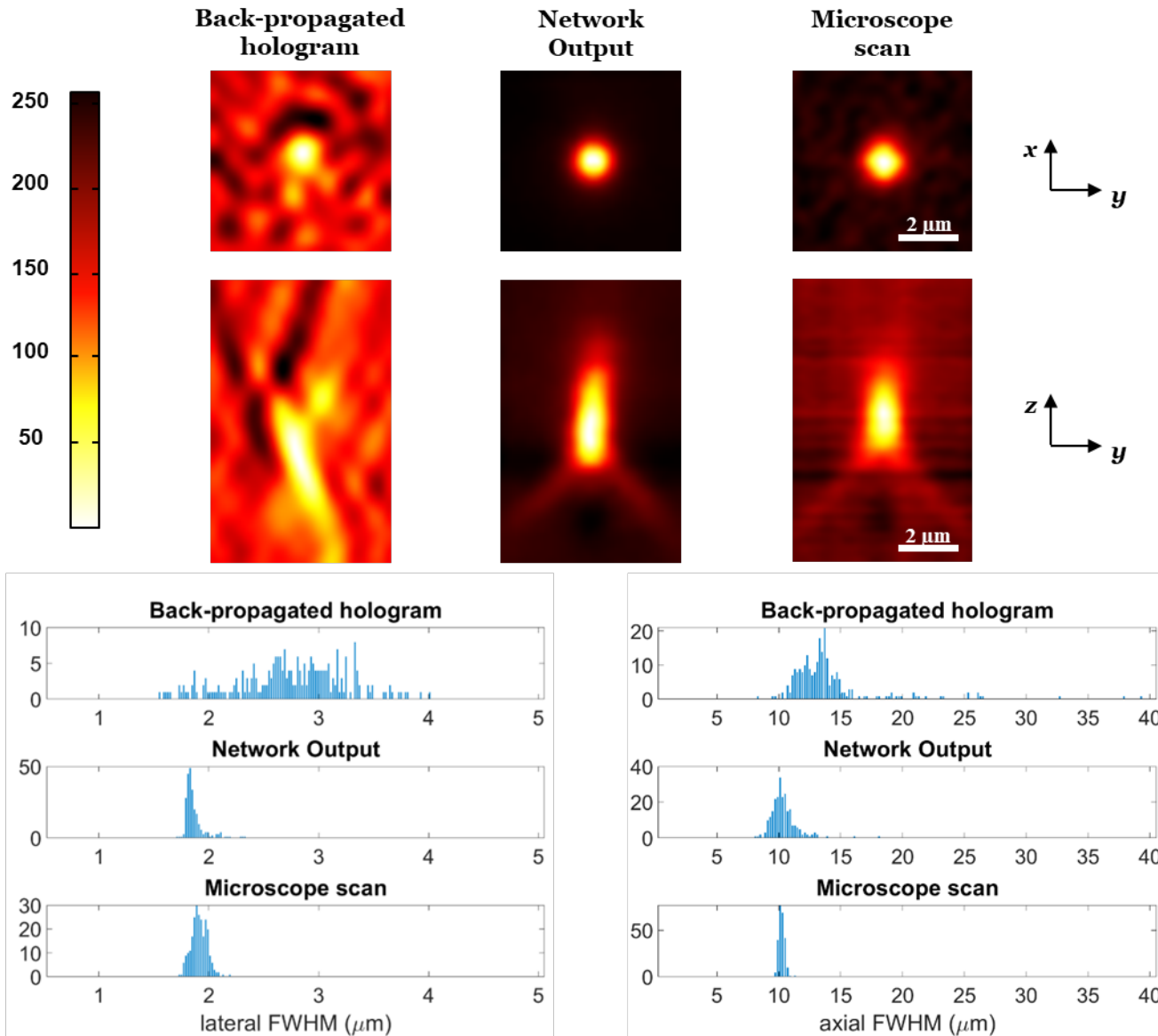
Cross-modality deep learning brings bright-field microscopy contrast to holography



Cross-modality deep learning brings bright-field microscopy contrast to holography



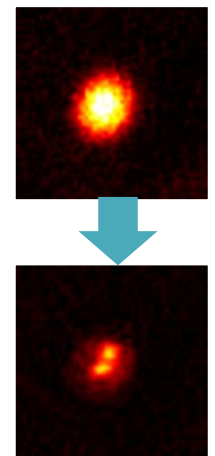
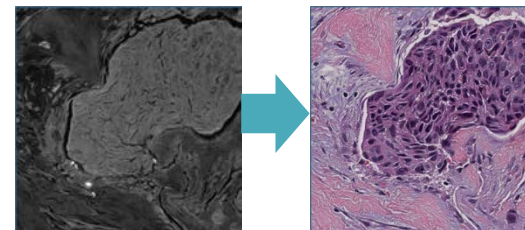
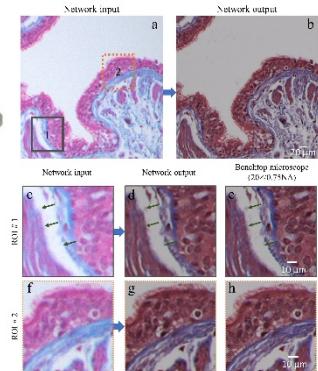
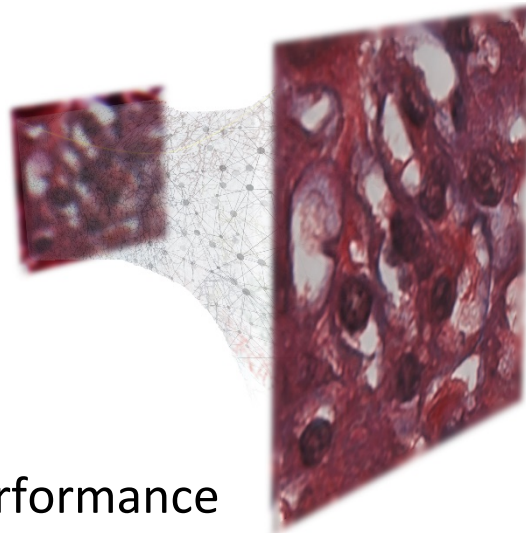
3D PSF comparison using 1 μm beads



Summary – enhanced microscopy

- Deep learning can substantially enhance microscopic images in terms of:

- Spatial resolution
- Field of view
- Depth of field
- Spectral distortions
- Compression
- Telemedicine
- Towards real time performance
- System characterization
- Virtual staining
- Virtual propagation



Optica 4, 1437-1443 (2017)
Light Sci. Appl. 7, e17141 (2018)
ACS Photonics (2018), DOI: 10.1021/acsp Photonics.8b00146
Nat. Methods 16, 103 (2019)
Nat. Biomed. Eng. 1 (2019). doi:10.1038/s41551-019-0362-y
Light Sci. Appl. 8, 23 (2019)
Light Sci. Appl. 8, 25 (2019)